Evaluating the Community Land Model in a pine stand with shading manipulations and $^{13}CO_2$ labeling

[Revised manuscript for Biogeosciences]

Jiafu Mao[1,*], Daniel M. Ricciuto[1], Peter E. Thornton[1], Jeffrey M. Warren[1], Anthony W. King[1], Xiaoying Shi[1], Colleen M. Iversen[1] and Richard J. Norby[1]

[1] Environmental Sciences Division and Climate Change Science Institute, Oak Ridge National Laboratory, Oak Ridge, Tennessee, USA

[*] Corresponding author: (Tel: +1-865-576-7815, maoj@ornl.gov)

Abstract. Carbon allocation and flow through ecosystems regulates land surface–atmosphere CO_2 exchange and thus is a key, albeit uncertain, component of mechanistic models. The Partitioning in Trees and Soil (PiTS) experiment-model project tracked carbon allocation through a young *Pinus taeda* stand following pulse-labeling with $^{13}CO_2$ and two levels of shading. The field component of this project provided process-oriented data that was used to evaluate terrestrial biosphere model simulations of rapid shifts in carbon allocation and hydrological dynamics under varying environmental conditions. Here we tested the performance of the Community Land Model version 4 (CLM4) in capturing short-term carbon and water dynamics in relation to manipulative shading treatments, and the timing and magnitude of carbon fluxes through various compartments of the ecosystem. When calibrated with pretreatment observations, CLM4 was capable of closely simulating stand-level biomass, transpiration, leaf-level photosynthesis, and pre-labeling ^{13}C values. Over the 3-week treatment period, CLM4 generally reproduced the impacts of shading on soil moisture changes, relative change in stem carbon, and soil CO_2 efflux rate. Transpiration under moderate shading was also simulated well by the model, but even with optimization we were not able to simulate the high levels of transpiration observed in the heavy shading treatment, suggesting that the Ball-Berry conductance model is inadequate for these conditions. The calibrated version of CLM4 gave reasonable estimates of label concentration in phloem and in soil surface CO_2 after three weeks of shade treatment, but lacks mechanisms needed to track the labeling pulse through plant tissues on shorter time-scales. We developed a conceptual model for photosynthate transport based on the experimental observations, and discussed conditions under which the hypothesized mechanisms could have an important influence on model

behavior in larger-scale applications. Implications for future experimental studies are described, some of which are already being implemented in follow-on studies.

1 Introduction

Accurate projection of the changing global climate, given a particular scenario of future greenhouse gas emissions or concentrations, is largely determined by adequate representation of mechanistic processes in Earth System Models (ESMs) (Taylor et al., 2012). Land Surface Models (LSMs) and their associated biogeophysical and biogeochemical parameterizations are key determinants of the ESMs' fidelity in characterizing and quantifying complex feedbacks in the Earth System (Arora et al., 2013; Friedlingstein et al., 2006; Pitman, 2003). Modeling studies have increasingly used observational data and mechanistic knowledge of processes to advance the development of LSMs (Best et al., 2011; Dai et al., 2003; Krinner et al., 2005; Oleson et al., 2013; Wang et al., 2011). Global and regional observations of land surface fluxes, states, and dynamic vegetation change offer insights into the large-scale interactions between the land surface and atmosphere, and hence facilitate model improvements at relevant scales in space and time (Beer et al., 2010; Huntzinger et al., 2012; Luo et al., 2012; Randerson et al., 2009). However, to better quantify and reduce uncertainties arising from deficiencies in model process representation, parameters, driver datasets and initial conditions, there has been significant effort to evaluate and to calibrate LSMs against site-scale observations and experimental manipulations (Baldocchi et al., 2001; De Kauwe et al., 2014; Hanson et al., 2004; Ostle et al., 2009; Raczka et al., 2013; Richardson et al., 2012; Schaefer et al., 2012; Schwalm et al., 2010; Stoy et al., 2013;

74 Walker et al., 2014; Williams et al., 2009; Zaehle et al., 2014). Further, model
75 development from these focused site-scale studies, especially in close collaboration with
76 experimentalists, can inform and prioritize new experiments and observations that are
77 specifically designed to advance understanding of critical terrestrial ecosystems and
78 processes (Shi et al., 2015).

79 The Community Land Model (CLM) is an advanced LSM with a comprehensive
80 mechanistic parameterization of carbon (C), water, and energy budgets for diverse land
81 types that can be applied across multiple temporal scales (Oleson et al., 2010). CLM has
82 been evaluated against observations from a wide range of sources, and these evaluations
83 have resulted in improved model performance (Bauerle et al., 2012; Bonan et al., 2011,
84 2012; Koven et al., 2013; Lawrence et al., 2011; Mao et al., 2012a, 2012b, 2013; Oleson
85 et al., 2008; Randerson et al., 2009; Riley et al., 2011; Shi et al., 2011, 2013, 2015;
86 Thornton et al., 2007). Nevertheless, little attention has been paid to CLM's ability to
87 replicate short-term manipulative experiments, which provide an avenue for exploring
88 and validating model response to sudden, large changes in environmental drivers that
89 control physiological and ecological responses (Amthor et al., 2001; Bonan et al., 2013;
90 Shi et al., 2015). Processes operating over short time scales can have long-lived
91 ecosystem consequences through indirect effects; e.g., stomatal conductance varies on
92 timescales of hours or shorter, but indirect effects on site-level water balance through
93 controls on transpiration can extend to annual timescales and beyond. Combined model-
94 experiment projects can focus efforts on specific mechanistic processes whose
95 representation in the model may be neither adequate nor appropriate for specific sites
96 (Walker et al., 2014; Zaehle et al., 2014). Extending these model-experiment evaluations

97 and ensuing model refinements to additional sites of the same and different ecosystem
98 types improves confidence in the regional and global scale adequacy of the LSM's
99 mechanistic process representation and parameterization.
100 Photosynthetic C assimilation, the allocation of photosynthetic products into
101 tissues with different turnover rates, and the respiration of C back into the atmosphere are
102 important determinants of CO_2 exchange between the terrestrial biosphere and the
103 atmosphere (Schimel et al., 2001). Biosphere-atmosphere C exchange is dynamically
104 mediated by weather, soil conditions, vegetation community composition and phenology,
105 and natural and anthropogenic disturbances (Cannell and Dewar, 1994; Litton et al.,
106 2007). Mechanistic characterization of the fate of photosynthetically-fixed C, in
107 particular the magnitude and timing of C allocation among plant compartments, is a
108 major challenge for experimental and modeling communities (Epron et al., 2012).
109 Various C-allocation schemes have been proposed and implemented in LSMs to capture
110 both the dynamic changes in C allocation and response to external conditions of C
111 allocation (De Kauwe et al., 2014). They generally employ either fixed coefficients or in
112 some cases dynamic coefficients that are functions of time or time-varying external
113 conditions to allocate assimilated C to different plant components (e.g., leaves, stems,
114 and roots). These allocation schemes and coefficients are generally not well constrained
115 by observations. More process-based understanding, better measurement techniques, and
116 targeted experimental manipulations are needed to better constrain allocation within the
117 model structure and the models' representations of C dynamics.
118 Carbon isotopes provide important constraints on specific processes and can be
119 used in labeling experiments to track pulses of carbon through plant and soil components.

120 Both diffusion through stomata and enzyme activity during photosynthesis discriminate
121 against the accumulation of ^{13}C in plant tissue, making ^{13}C measurement a useful
122 constraint on stomatal conductance (Farquhar et al., 1989). Exposing plants to ^{13}C
123 enriched CO_2 can provide important constraints on simulated C allocation (Ehleringer et
124 al., 2000). The post-treatment carbon isotope composition ($\delta^{13}C$) of organic matter and
125 respired CO_2 can serve as a tracer of plant C allocation (Atkin 2015; Bahn et al., 2012).
126 We evaluated the integrated response of a simulated tree-soil system to an
127 imposed alteration of shortwave radiation, the main environmental driver for
128 photosynthesis, and compared the observed trajectory of labeled carbon pulses through
129 that system with approximations of carbon allocation that are typical of a global-scale
130 model. We used a version of CLM4.0 that has been modified to allow convenient
131 application of the global-scale modeling algorithms at single points (PTCLM, described
132 in Oleson et al., 2013). We evaluated the model against observations and experimental
133 results from the "Partitioning in Trees and Soils" (PiTS) experiment established in a
134 young loblolly pine stand in Oak Ridge, Tennessee, USA (Warren et al., 2013). The
135 project exposed a young loblolly pine (*Pinus taeda*) stand to a pulse of air enriched with
136 $^{13}CO_2$, then tracked that label from photosynthetic uptake, through the leaves, stem, and
137 roots and ultimately out of the soil as respiratory flux (Warren et al., 2012). We addressed
138 two questions: (i) Is the model able to represent the biophysical and ecophysiological
139 behavior of the experimental system in terms of pretreatment dynamics and stand-level
140 response to the manipulated radiation environment? (ii) Do the biases inherent in a very
141 simple model of storage and allocation propagate beyond the time scale of fast turnover
142 storage pools? We hypothesized that it would be possible to parameterize the global

143 model using site-level ecophysiological measurements, and have it realistically capture
144 the site-level influence of the shade manipulation. We further hypothesized that, in spite
145 of missing mechanisms to track short-term storage and allocation of C, the parameterized
146 model could capture both pretreatment ^{13}C discrimination as well as post-treatment
147 effects once the labeling pulse had traveled through the plant.
148

149 2 Methodology

150 2.1 Site description, experimental manipulation, and observations

151 The field component of the project was conducted in a young loblolly pine stand at the
152 University of Tennessee Forest Resources AgResearch and Education Center in Oak
153 Ridge, Tennessee. The soil is classified as a silt-clay-loam (13.3% sand; 35.7% clay;
154 51.0% silt), with bulk density ranging from 1.2 to 1.4 g cm^{-3} at 10 to 70 cm depth. One-
155 year-old seedlings (1 g C m^{-2} (Griffin et al., 1995)) were planted at 2.5 × 3 m spacing in
156 2003, and the experiment was conducted in 2010 when the trees were ~7 m tall.
157 In 2010, a subset of eight of the trees, adjacent to one another, and their soils, were
158 instrumented with automated sensors to continuously measure soil temperature, soil
159 moisture vertically throughout the soil profile, soil surface $^{12}CO_2$ and $^{13}CO_2$ efflux, root
160 production at 10 and 30 cm depths, stem sap flow, and stem diameter (Warren et al.,
161 2012). Various measurements were manually collected periodically, including predawn
162 foliar water potential, photosynthetic light- and CO_2-response curves, root biomass,
163 growth, and mortality, and soil C and nutrient content. Meteorological data were
164 collected every 30 minutes at 2 m height in an adjacent open field, and included wind

165 speed, air temperature, photosynthetically active and shortwave radiation, precipitation,
166 and relative humidity.

167 Following several weeks of pretreatment measurements, the eight study trees
168 were enclosed with plastic film stretched over a frame surrounding the trees, and then
169 trees were exposed to 53 liters of 99 atom % $^{13}CO_2$ for 45 minutes. The plastic was
170 removed and replaced with light shade (LS) or heavy shade (HS) cloth, each of which
171 covered four trees and provided differential levels of photosynthetically active radiation
172 (PAR) at the canopy surface for 3 weeks following the labeling. The LS and HS cloths
173 were designed to allow passage of 70% and 10%, respectively, of the incident PAR.

174 To assess actual conditions under the shade cloth treatments, short-term
175 measurements of temperature, humidity, wind speed, and PAR were collected at the
176 canopy surface following shade cloth installation. Linear regressions between
177 meteorological data from under the shade cloth and from the open field were used to
178 estimate conditions at the canopy surface during the experimental period. Temperature
179 was ~0.11°C (± 0.82 °C; ± 1 *SD*) lower, relative humidity (H_r) was ~6% (± 5%; ± 1 *SD*)
180 higher, and wind speed (u) was ~45% (± 15%; ± 1 *SD*) lower, under both levels of
181 shading than in the adjacent open field (Fig. 1a, b). The shade cloths performed very
182 close to design, with 68% and 11% passage of PAR through the LS and HS cloths,
183 respectively (Fig. 1c).

184 Non-destructive measurements of soil moisture, soil temperature, soil respiration,
185 sap flow and stem growth were made prior to the labeling and for the duration of the
186 shade treatment. During the shade treatment, destructive measurements of foliage, stem
187 phloem tissue, roots and soil were collected to assess presence of the ^{13}C label, and linked

188 to concurrent automated measurements of $^{13}CO_2$ from the soil surface (Warren et al.,
189 2012). Experimental results and additional details on the site and experimental design are
190 in Warren et al. (2012) and datasets are available online (Warren et al., 2013).

191 2.2 Model description

192 We used CLM4 (Oleson et al., 2010), the land component of the Community Earth
193 System Model (CESM) (Gent et al., 2011), to simulate the pretreatment and manipulated
194 processes in the PiTS study. This CLM version includes fully prognostic carbon and
195 nitrogen representations for its vegetation, litter, and soil biogeochemistry components
196 (Oleson et al., 2010, 2013; Thornton et al., 2007; Thornton and Rosenbloom, 2005).
197 Carbon allocation in this version of CLM is simplistic. After maintenance
198 respiration demands are calculated and subtracted from gross primary productivity
199 (GPP), and following a step that downregulates GPP on the basis of static allocation
200 parameters, fixed tissue C:N stoichiometry, and plant mineral N uptake, the available
201 carbon is allocated to new growth, storage for growth in subsequent growing seasons, and
202 associated growth respiration. The model includes pools for leaf, fine root, and several
203 categories of stem and coarse root, with over-season storage pools associated with each
204 of these "displayed" growth pools. The allocation ratio between stem and leaf is a
205 function of the previous year's net primary productivity (NPP; higher fractional
206 allocation to stem with higher annual NPP), while all other allocation ratios are fixed
207 throughout the simulation for a given vegetation type. For ^{13}C, stomatal diffusion and
208 photosynthetic fractionation are calculated and photosynthetically fixed ^{13}C is
209 immediately allocated to plant pools following the above description. There is no further
210 fractionation in within-plant processes or during decomposition (Oleson et al., 2013).

Several major developments of CLM performed specifically for this study include: (1) introducing the ability to represent the shade effect and experimental labeling by driving the model with observed atmospheric $^{13}CO_2$ concentrations, where before $^{13}CO_2$ was assumed to be a constant fraction of CO_2, (2) developing a site-level simulation workflow that leverages PTCLM capability to reproduce actual field experiments, (3) calibration of the selected model parameters to improve predictions and reveal structural errors, and (4) adding a stand-alone testing capability for the photosynthesis subroutines.

2.2.1 Description of PTCLM simulation

To perform simulations at the PiTS site, we used PTCLM, a scripting framework to run site-level simulations of CLM efficiently with site-specific forcing and initialization data (Oleson et al., 2013). We performed the standard 600 years of accelerated decomposition spinup, in which soil organic matter decomposition rates are increased (Thornton and Rosenbloom, 2005), followed by 1000 years of normal spinup, in which the decomposition rates are returned to their normal values, and a transient simulation between 1850-2010 using historically varying CO_2, $^{13}CO_2$, nitrogen deposition, and aerosol forcing data. Long-term meteorological driver data were not available at the PiTS site, and instead were taken from the nearby Walker Branch and Chestnut Ridge eddy covariance sites (Hanson et al., 2004) for the years 2000-2010. These input data were cycled continuously to drive the model through the spinup and transient simulations. On model date 1 January 2003, we simulated a harvest disturbance by removing existing vegetation biomass and simulating planting of seedlings using a biomass of 1 g C m^{-2}. The model then simulated growth of the young stand through the year 2010. For the

234 spinup and transient phases through 2002, default temperate evergreen needleleaf model
235 parameters were used. Beginning in 2003, model parameters were modified to simulate
236 the planted loblolly trees, based on ecophysiological measurements and model calibration
237 (see Section 2.2.2).

238 To simulate the treatment period, we replaced the meteorology from the eddy
239 covariance sites with observed data at the treatment sites starting at day of $^{13}CO_2$ labeling
240 in September 2010 (Warren et al., 2012). The $^{13}CO_2$ pulse was applied in the model
241 (assuming 100% $^{13}CO_2$) during a time matching the labeling period. Thermal infrared
242 camera measurements under both light and heavy shade cloth made during various sky
243 conditions indicated the need to modify the model input for incoming longwave radiation
244 under the heavy shade treatment, by assuming that the heavy shade cloth emitted
245 downward longwave at a blackbody temperature equal to the open field air temperature
246 (data not shown). For the light shade case, we applied the model's internal estimate of
247 incoming longwave radiation, which uses clear-sky assumptions about atmospheric
248 temperature and emissivity (Idso, 1981).

249 2.2.2 Model calibration for pre- and post-treatment periods

250 Model evaluations are complicated by the co-occurrence of parametric and structural
251 uncertainty, which confounds the attribution of model errors (Keenan et al., 2011). A
252 model's performance might be negatively impacted by misrepresentation of mechanistic
253 processes, poor parameterization of otherwise sound functional representations, or both.
254 Parameter optimization, however, can help to isolate structural deficiencies in the model.
255 In this study, we applied model calibration, by optimizing model parameters, as a tool to
256 highlight areas for model development rather than simply improving predictive skill. We

257 optimized selected CLM parameters against pretreatment data. We then evaluated the
258 performance of the calibrated CLM in the pretreatment phase and again in the post-
259 treatment phase without recalibration following simulation of the canopy shading and
260 $^{13}CO_2$ treatments. Our intention is that by applying robust parameter optimization to the
261 pretreatment simulations we will reduce parametric uncertainty (Fox et al., 2009;
262 Ricciuto et al., 2011), leading to greater insight regarding model structural uncertainty in
263 evaluation of the post-treatment results.

264 We first calibrated the model to simulate the pretreatment conditions using
265 observations and prior information about model parameters. Data constraints for the
266 calibration consisted of single pretreatment estimates for leaf, stem, and root biomass
267 from allometric relationships for similarly aged loblolly pine (Baldwin, 1987; Naidu et
268 al., 1998; Vanlear et al., 1986), a pretreatment $\delta^{13}C$ measurement for leaves, a
269 pretreatment $\delta^{13}C$ measurement for bulk roots, and daily sap flow and soil respiration
270 observations from each of the 20 days preceding the $^{13}CO_2$ labeling and shading
271 treatments. Because CLM predicts canopy transpiration but not sap flow, daily
272 transpiration during the experiment was estimated by scaling the sap flow measurements
273 using sapwood area and ground area covered by the rooting system (Wullschleger et al.,
274 2001; Warren et al., 2011). Here we assume the rooting system of each tree occupied 7.5
275 m^2 of ground area based on the spacing between the trees. For consistency, sap flow is
276 hereafter called transpiration for both the observational and modeled results.

277 Some model parameters were measured directly from observations (Table 1).
278 Other parameters for which direct estimation was not possible were optimized to
279 maximize fit between model results and the observed calibration data (Table 1). The

selection of parameters for optimization was based on formal sensitivity analysis (Sargsyan et al., 2013) and prior experience with the model. We defined the sum of squared errors (SSE) between simulation and observations weighted by data uncertainty as the cost function for the optimization. We used a genetic algorithm (Runarsson and Yao, 2000) to find a set of parameters that minimizes the cost function. Simulations were performed in parallel using 2 populations of 32 ensemble members in parallel over 100 iterations for a total of 6400 model simulations.

For the pretreatment (pre-labeling) period, we compared the standard 'parameter' version of the model (PRE-STD) with the optimized 'parameter' version (PRE-OPT). The model with optimized parameters was used in simulations for the shading treatment period for both the high shade and low shade treatments. Because of uncertainties associated with simulated stomatal conductance and transpiration in high-shade conditions, we performed additional parameter calibrations for the parameters mp (slope of the Ball-Berry stomatal conductance formulation) and bp (intercept of the Ball-Berry stomatal conductance formulation) during the shade treatment period using the genetic algorithm with transpiration and stem growth data as constraints (HS_MB), with results discussed below.

2.2.3 Evaluation of CLM photosynthesis functions

Since we are interested in understanding the fate of photosynthetically fixed carbon as it is allocated to various tissues and fluxes, and how allocation dynamics respond to changes in photosynthesis as driven by changes in PAR, it is useful to evaluate model predictions of photosynthesis over a range of light levels. We used a functional unit testing framework (Wang et al. 2014) to evaluate CLM's representation of the

303 photosynthetic light response at the scale of individual leaves against light-response
304 curves obtained by Warren et al. (2012) for foliage in the upper canopy of trees at the
305 PiTS experimental site prior to the shade treatment. This approach isolates the targeted
306 model process to allow a direct comparison between instrumental data and simulation
307 output, driving the model component with specified environmental conditions and
308 parameter values.
309

310 3 Results

311 3.1 Environmental forcing conditions

312 Mean surface air temperature adjacent to the site decreased from days -20 to 4 (day
313 numbering is negative prior to the addition of $^{13}CO_2$ and shading treatments), then
314 recovered somewhat and remained without obvious trend for the rest of the post-labeling
315 period (days 5 to 25). Multiple rainfall events were recorded in the pre-treatment and
316 treatment periods (Fig. 2a). The shortwave and longwave radiation drivers for our
317 simulations, based on a combination of observations and estimation as described above,
318 showed variance associated with weather patterns during the experiment, with the
319 superimposed influence of the light and heavy shading treatments (Fig. 2b). $^{13}CO_2$
320 concentrations followed historical background values except during the labeling period
321 on day 0 (Fig. 2b).

322 3.2 Pretreatment and treatment evaluation

323 The model predicted approximately exponential growth in all biomass pools during the 8
324 years of pretreatment simulation, with some evidence of slowing growth in the final years
325 (Fig. 3a). Using default global-scale ecophysiological parameters, the model significantly

326 overestimated biomass accumulation in leaf, stem, and root pools, by 85%, 36%, and
327 76%, respectively on Sep. 1st of year 2010 (PRE_STD curves, Fig. 3a). Replacing default
328 parameters with observed (lower) leaf N concentration and with calibrated (higher)
329 allocation ratios for stem:leaf and root:leaf (complete set of parameter changes shown in
330 Table 2) brought the biomass accumulation curves in better agreement with observations
331 (Fig. 3a). Using the PRE_OPT parameters, the bias for leaf, stem, and root biomass
332 accumulations was -9%, -4%, and -16%, respectively, compared to observed values.
333 Comparison of predicted vs. observed photosynthesis light response curves was
334 used as an independent assessment of the model performance before and after calibration
335 across a range of PAR values characteristic of mid-day values in the open field and under
336 the LS and HS treatments (Fig. 3b). In the range of PAR from 750 to 1588 μmol m^{-2} s^{-1},
337 typical of mid-day conditions in the pre-treatment period (days -25 to -1), default
338 parameterization (PRE_STD) resulted in overestimates of photosynthesis, while data-
339 constrained and calibrated parameterization (PRE_OPT) eliminated the bias, placing
340 predictions within +/- 1 SD of observed values. For light conditions characteristic of mid-
341 day values in the LS treatment (648 +/- 232 μmol m^{-2} s^{-1}) the overprediction bias for the
342 optimized model was reduced, but at PAR = 500 μmol m^{-2} s^{-1} the optimized model
343 predicted photosynthesis was still biased high. For the range of PAR characteristic of the
344 HS treatment (131 +/- 47 μmol m^{-2} s^{-1}) the model with optimized parameters
345 underestimated photosynthesis, while the model with default parameters was in good
346 agreement (low end of the range) or was biased high (high end of the HS range).
347 Soil temperature predicted by the optimized model at 0-5 cm depth had a
348 consistent overestimation bias of 1-2 °C, but the model closely reproduced the daily

349 variation and decreasing tendency in near-surface soil temperature in both the
350 pretreatment and post-treatment periods (Fig. 4a). No clear influence of shading
351 treatments on soil temperature was seen in either the observations or model simulations.
352 Substantial variability in observed soil moisture (integrated for 15-95 cm depth) was
353 found among samples taken near different trees under the same shading treatment (Fig.
354 4b). Pretreatment observations of soil water content were not made, but observed LS soil
355 water was lower than that of the HS soil water at the start of the treatment period, perhaps
356 reflecting local differences in soil properties and pretreatment evapotranspiration.
357 Although modeled soil water content at the start of the treatment was higher than
358 observed (by 5-7%, measured as volume % of water in soil), the maximum observed and
359 simulated excursions in soil water content between rain events during the treatment
360 period were similar (4% and 3.5%, respectively). Predicted soil water content declined
361 more slowly than observed during days 16-25. There is some evidence of both observed
362 and predicted LS water content declining more rapidly than HS in this same period,
363 suggesting higher rates of evaporation for LS than HS.
364 Observed transpiration during the pretreatment period was higher for HS than LS
365 plots, likely a consequence of the higher biomass and leaf area of the HS trees (Warren et
366 al., 2012) and perhaps also higher soil water content (Fig. 4b). We used the pretreatment
367 transpiration data to calibrate CLM, and the model simulated the pretreatment
368 observations well in terms of both magnitude and temporal variations (Fig. 4c). After the
369 treatment initiation, decreased transpiration was seen in both observations and model
370 simulations for the HS and LS trees. For the LS case, CLM captured the observed
371 transpiration well. However in the HS case, CLM predicted a sharp reduction in

372 transpiration, whereas the observations differed relatively little from the LS case. To
373 investigate this difference further, we performed a second optimization for the Ball-Berry
374 stomatal conductance slope and intercept terms (HS_MB). However, despite increasing
375 these parameters to near the maximum acceptable values (Table 1), the HS_MB
376 optimization failed to reproduce the measured transpiration.
377 Both HS and LS trees showed increasing trend in stem carbon during the
378 pretreatment period, as inferred from stem thickness measurements. While the LS stems
379 continued to grow during the treatment period, the observed HS stem size declined (Fig.
380 5a). Modeled relative increase in stem carbon was more rapid during the pretreatment
381 period than observed, and while the modeled LS trees continued to accumulate carbon
382 during the treatment period (at a somewhat reduced rate) the modeled HS tree growth
383 essentially stopped. The observed shorter-term (3-5 day) variation in stem carbon (based
384 on diameter change) under shading (Fig. 5a) was attributed primarily to precipitation
385 events and changing soil moisture (Fig. 2a and Fig. 4b), and the accompanying swelling
386 and shrinkage of stem diameter, which translates through the allometric functions to
387 apparent changes in stem biomass. Apart from whole-plant mortality and fire, the model
388 has no physiological mechanisms allowing for negative growth of stems.
389 Both observed and simulated soil respiration tended to decline over the study
390 period (after Day-10 in the observations) (Fig. 5b). The observed pretreatment soil
391 respiration beneath the trees chosen for the HS treatment was 30% higher than under
392 those selected for the LS treatment. After the application of the shade treatments, relative
393 differences between the observed HS and LS soil respiration were reduced, but
394 respiration from HS soil remained higher. In contrast, simulated soil respiration was

slightly higher under LS, although the difference is quite small. The observed short-term variability in soil respiration under both HS and LS was not well simulated. While observations showed a reduced soil respiration coinciding with large precipitation events around Days -10, +10, and +15, simulated soil respiration rose on those days.

3.3 ^{13}C evaluation

Observations of foliar $\delta^{13}C$ show that LS and HS leaves acquired a similar concentration of labeled C, as intended by the experimental design (Fig. 6a). Observed appearance of the labeled C in phloem shows that photosynthate was rapidly moved out of leaves and into phloem, with peak observed phloem concentrations on day 2 for both LS and HS trees (Fig. 6b). Labeled C was observed in CO_2 at the soil surface, with peak concentrations around day 4 indicating a transfer through phloem to roots and metabolism belowground either as root respiration or as heterotrophic respiration of root exudate or root tissue (Fig. 6d). Increase in labeled C was observed in root tissue for both LS and HS trees, with large variability in measurements (Fig. 6c). Leaf, phloem, and root tissues showed remaining labeled C at day 20, and the label was still evident in soil surface CO_2 at day 15. For both phloem and soil surface CO_2, the LS plots showed lower label concentrations than the HS plots throughout the observed rise and fall of the labeled pulse. Differences between label dynamics for LS and HS roots are difficult to assess due to variability in measurements.

The model reproduced observed pretreatment values for foliar, phloem, and root tissue $\delta^{13}C$, and for $\delta^{13}C$ in soil CO_2 flux to within 1.5‰ (Fig. 6), indicating reasonable model parameterizations for ^{13}C discrimination through the stomatal conductance and photosynthesis pathways. The model allocation approach deploys new photosynthate

418 immediately throughout the plant to meet current maintenance and growth respiration
419 demands. The belowground component of the modeled autotrophic respiration is seen as
420 a large spike in labeled C in soil surface CO_2 on day 0. Other similar spikes were
421 simulated in association with respiration of aboveground plant parts (results not shown).
422 Lacking a representation for multi-day transport of photosynthate to sites of growth,
423 either acropetally towards new canopy growth or basipetally towards stem or root
424 growth, the model allocates labeled C to new growth pools immediately, where it is
425 considered well-mixed with the existing plant tissues. There was thus a rapid increase and
426 then a relative stabilization of the $\delta^{13}C$ label in foliage and root tissue. The model does
427 include storage pools, which hold photosynthate for deployment as new growth in
428 following growing seasons. Those pools were lumped for comparison to the phloem
429 observations (Fig. 6b), and they followed a pattern similar to the predicted leaf and root
430 tissue pools.
431 The model predicted a steady dilution of labeled C in leaf, root, and storage pools
432 for the LS trees, compared to their HS counterparts. With a severe reduction in PAR,
433 GPP was greatly reduced in the modeled HS treatment, and what little photosynthate
434 produced was prioritized for maintenance respiration, so the label appeared quickly in
435 tissues and remained relatively constant for that treatment. For the LS treatment GPP
436 remained relatively high following the labeling and initiation of the shade treatment. In
437 this case unlabeled C continued to accumulate as new growth, causing a steady decline in
438 the label concentration for LS trees over the course of the experimental period (Figs.
439 6a,b,c, insets). In contrast to the plant pools, modeled soil surface CO_2 shows a gradual
440 increase in label concentration after the initial root respiration pulse on day 0, with HS

441 consistently showing a higher concentration of label than LS for the simulated soil
442 surface CO_2 through the end of the treatment period (Fig. 6d, inset). The modeled process
443 of leaf and fine root litterfall is continuous throughout the year for evergreen vegetation,
444 and this modeled rise in soil surface CO_2 concentration of labeled C is due to litterfall and
445 subsequent metabolism by heterotrophs.
446 Toward the end of the experimental period, the observed multi-day pulses of
447 labeled C in phloem and soil surface CO_2 approached the relatively stable values
448 predicted by the model. The observed trajectory for label concentration in leaves fell
449 below modeled values for the final ten days of treatment. Variation in observed root label
450 concentration toward the end of the experiment makes it difficult to assess
451 correspondence with model results for that tissue.
452

453 4 Discussion

454 4.1 Assessment of model performance in pretreatment period

455 Default model physiological parameters most appropriate to our site are based on
456 averages taken across numerous datasets collected in evergreen needleleaf forests. There
457 is considerable variation within that broad type classification for all of the measured
458 parameters (White et al. 2000), and any time a site-level evaluation is used to assess
459 model behavior (as here) it is helpful to constrain within this range according to the local
460 species or species mixture. We used measurements taken directly from the site where
461 available, and constrained the optimization of other parameters based on the observed
462 ranges for loblolly pine, when available. The fine-root to leaf allocation ratio increased
463 from 1.0 to 1.24, which is well within the range of reported values (White et al., 2000).

464 The fraction of leaf nitrogen in RuBisCO was 70% higher than the model default value,
465 and while on the high end, is consistent with measurements of other loblolly pine trees
466 (Tissue et al., 1995). The temperature sensitivity of maintenance respiration (Q_{10mr})
467 nearly doubled from the default value of 1.5 to 2.83. This is higher than most values in
468 the literature but is consistent with the value of 2.71 reported by Hamilton et al. (2001)
469 for loblolly pine, although this value only pertains to leaf respiration. The optimized
470 value for stem to leaf allocation ratio also is higher than in the default model, but it falls
471 well within the observed range for loblolly pine (White et al. 2000).

472 The optimized model delivered very reasonable simulations of pretreatment tree
473 biomass, transpiration, and leaf $\delta^{13}C$ (Figs. 3a, 4c, and 6a). Including multiple
474 independent observational metrics in the optimization cost function is a more challenging
475 test of correct model structure, compared to optimization targeting a single model output
476 variable (Sacks et al. 2006; Richardson et al., 2010; Ricciuto et al., 2011). The fact that
477 our optimized model delivers good results for all three components simultaneously
478 (biomass, transpiration, and leaf $\delta^{13}C$) supports the notion that stand-scale model
479 structure is reasonable.

480 Independent evaluation of model results at the leaf-scale demonstrated that the
481 optimized parameters either reduced biases (LS and open-field light levels) or gave
482 mixed results (HS light levels) at this scale. This provides additional confirmation that the
483 optimization approach was reasonable, and was not generating unrealistic parameter
484 values to compensate for gross structural deficiencies in the model. This is further
485 confirmed by the fact that optimized parameters (Table 1) controlling stomatal
486 conductance changed only modestly from default values.

Independent evaluation of model against pretreatment $\delta^{13}C$ in phloem and in soil surface CO_2 shows good agreement, consistent with the targeted pretreatment value for $\delta^{13}C$ in leaves. Simulated bulk root $\delta^{13}C$ is biased slightly high (Fig. 6c), indicating possible errors in root turnover time, or the model's failure to account for post-photosynthetic fractionation (Badeck et al., 2005).

Though several changes in the canopy photosynthesis scheme were made in the version 4.5 of CLM (Bonan et al., 2011; Oleson et al., 2013), in this work, the canopy photosynthesis process of CLM4.0 did a reasonably good job against our evaluation metrics, including the leaf-level light response data. The ability of our optimized model to reproduce pretreatment biomass, transpiration, ^{13}C discrimination, and leaf-scale photosynthetic response to light gives confidence in the model's ability to simulate the shading effect, and the model's ability to scale leaf-level processes to growth at the whole-tree scale.

4.2 Assessment of model performance in treatment period

We did not attempt to optimize model predictions for soil temperature or soil moisture content. The model overestimation of soil temperature while faithfully reproducing the multi-day excursions in temperature is consistent through the pretreatment and treatment periods. Soil surface temperatures were not measured, so it is not clear if the overestimation bias is related to a surface energy balance bias, to a bias in the overlying air temperature, or to parameterization error in thermal diffusivity and its relationship to soil texture and surface layer properties.

The overestimation bias in modeled soil moisture during the treatment period (there were no pretreatment observations) suggests a parameterization error for soil

texture or variation in texture with depth. Small differences in the clay fraction, for example, could cause the observed offset in mean soil water content, and clearly there is variability in soil moisture states across the site, both within and between the shade treatments (Fig. 4b). We used a single estimate of sand, silt, and clay fractions from the site, and were satisfied that the model was able to capture pretreatment transpiration with that soil parameterization, and that the multi-day excursions of soil moisture were of similar magnitude in the model compared to observations during the treatment period. We also note that modeled stomatal conductance was not impacted by lack of soil water in these simulations. Periodic rainfall kept soils relatively wet throughout the pre-treatment and treatment periods, minimizing effects of bias in soil moisture on simulated photosynthesis or transpiration.

The very large difference between modeled and measured transpiration for the HS treatment is the most confounding result from our study. The model carbon and water dynamics are well-behaved for the pretreatment period, and the model also captures the influence of light shading on transpiration accurately. Stem growth results indicate that reduced growth of LS trees, and the cessation of growth for HS trees, is captured properly by the model. Through the Ball-Berry approximation linking stomatal conductance to photosynthetic rate, the model is forced into a state of reduced transpiration for the HS treatment, even with additional optimization that placed Ball-Berry parameters at their outer observational limits. It is possible that the sapflow measurements in the HS treatment are biased, and that the actual tree-scale transpiration is not as high as suggested by these measurements, but if true we would expect that bias to occur for both pretreatment and treatment periods, and not only to appear in the treatment period, as

observed. Connected to that hypothesis, it is possible that actual leaf stomatal conductance shut down during the HS treatment, but that water continued to accumulate in the stem, moving past the sapflow sensors and filling a capacitance in the xylem tissue. However, the sustained sapflow over the long duration of the treatment period and the negative observed trend in stem diameter for HS trees argue against that interpretation.

Alternatively, if we assume that the sapflow measurements reflect actual high levels of transpiration in the HS trees, then we are forced to conclude that the Ball-Berry relationship as implemented in CLM (De Kauwe et al., 2013; Oleson et al., 2010, 2013) breaks down under these rather extreme experimental conditions. Under that hypothesis, it would seem that there is some "memory" of the expected range of light levels in the tree, and that even when photosynthesis is nearly extinguished due to experimentally forced reduction in PAR, stomatal conductance remains at a relatively high level. Another possibility is that these trees exhibit a strong nonlinearity in the relationship between stomatal conductance and net photosynthesis, which has been observed at low light levels and strongly impacts estimated transpiration (Barnard and Bauerle, 2013). This type of nocturnal transpiration may indeed have been greater for the HS trees if the vapor pressure deficit was larger (Domec et al. 2012). Errors in modeled leaf temperature and leaf boundary layer vapor pressure deficit may also contribute to the discrepancy with observations. Conductance may have been maintained to some extent by vapor pressure differences between the foliage and the shade cloth – indeed, dew was observed on unshaded trees in early morning, yet not on the shaded trees. This hypothesis could be tested in future studies with additional leaf-level measurements under HS treatments, sampling both the diurnal cycle and the multi-day behavior of leaf physiology in trees

556 subjected to high levels of shading. While the HS conditions are unlikely to be realized
557 for extended periods under natural conditions, understanding this failure of the
558 commonly-used Ball-Berry parameterization may be helpful in understanding and
559 predicting the broader case of adaptation of stomatal behavior to environmental change,
560 which is known to influence water and carbon cycle predictions under future climates
561 (Damour et al., 2010).

562 Stem diameter can shrink or swell based on changes in stem xylem water content,
563 bark water content, and cambial growth, and is dependent on xylem water potential,
564 vapor pressure deficit, C availability, non-structural carbohydrate concentrations, and C
565 allocation (Vandegehuchte et al., 2014). C allocation to stem growth is revealed by a
566 step-wise increase in stem diameter that occurs in response to favorable conditions, and
567 that is maintained under less favorable conditions. The LS treatment clearly displayed the
568 step-wise increases in stem diameter, while the HS treatment displayed a reduction in
569 stem diameter. The shrinking stem diameter of HS trees indicates a decline in xylem and
570 phloem water content likely linked to phloem sugar concentration. The HS treatment
571 certainly reduced foliar C uptake and C available for phloem loading and allocation to
572 cambial growth (Warren et al., 2012).

573 The modeled difference between LS and HS in biomass accumulation in stems is
574 in good agreement with observations based on stem diameter, with increases of 1.9% and
575 1.6% by treatment day 19 for model and observations, respectively (Fig. 5a). Given the
576 previously discussed pretreatment results for biomass accumulation and leaf-scale
577 photosynthesis, we are confident in the optimized model's ability to capture carbon
578 dynamics at the plant scale on time scales of years to tens of days. It is reassuring to see

579 that the model prediction of soil respiration falls in the observed range, although this
580 could be the result of good luck as much as good performance. While soil respiration on
581 an annual basis is closely related to litter inputs and belowground plant respiration, it is
582 possible for compensating errors between decomposition rates and litter inputs, or
583 between litter inputs and root respiration, to result in good model-observation agreement
584 for the approximately monthly timescale examined here. We note a potential bias in the
585 model relationship between soil respiration and soil moisture: while the observed soil
586 respiration is depressed after large precipitation events, the model estimates an increase.
587 Neither CLM4's carbon allocation to roots nor its predicted root respiration is dependent
588 on soil water conditions. CLM4's heterotrophic contribution to soil respiration may also
589 have too little sensitivity and the timing of soil respiration response to soil water variation
590 may also be too simplistic. A more mechanistic treatment of water-air-microbe
591 interactions at the scale of soil pore space might help to eliminate these differences.
592 Resolved vertical transport of respired CO_2 in the soil column might also help to correct
593 this bias.

594 Beyond noting the obvious discrepancy in observed vs. modeled $\delta^{13}C$ dynamics
595 associated with the lack of short-term photosynthate storage pools in CLM, we are
596 interested in using this study to develop hypotheses explaining the observed patterns in
597 $\delta^{13}C$, identifying the simplest mechanisms that explain observed patterns, and
598 understanding the consequences of ignoring those mechanisms in a model like CLM. To
599 the extent that simple mechanisms can be identified, and significant consequences of
600 ignoring those mechanisms articulated, we leave it to future efforts to deploy and

601 evaluate those mechanisms in new model versions and with new observational and
602 experimental constraints.
603 Given that LS and HS leaves seem to have photosynthesized the pre-shading
604 labeled pulse of CO_2 at similar rates (Fig. 6a) as intended by the experimental design, we
605 can make some inferences about the dynamics of photosynthate storage and transport
606 based on the timing of the pulse as it exits the foliage and passes through the phloem of
607 the trunk, and based on differences in timing and concentration of the labeled pulse in LS
608 and HS trees. First, the fact that observed peak label concentration is higher in phloem
609 than in foliage, even though that peak comes two days later in phloem than in foliage,
610 indicates that the phloem pool in the vicinity of the labeling source (the leaf) is smaller
611 than the leaf pool itself. That is, even though the label is passing into the leaf prior to
612 entering the phloem, the label pulse is relatively small compared to the leaf carbon pool
613 as a whole, while it is relatively large compared to the part of the phloem pool nearest the
614 leaf at the time of labeling. Second, the observation that $\delta^{13}C$ in foliage declines rapidly
615 over the first ten days, and declines at about the same rate for LS and HS leaves, indicates
616 that the movement of newly-fixed photosynthate from leaves and into phloem does not
617 depend strongly on production of new photosynthate in subsequent days. Third, the
618 similar timing between LS and HS trees for peak label concentration in phloem, and later
619 in soil surface CO_2, indicates that the velocity of material movement through the phloem
620 does not depend strongly on current photosynthesis rate. Since the HS treatment clearly
621 reduced growth and transport belowground (Fig. 5), the logical conclusion is that the
622 cross-sectional area of active phloem tissue responsible for transport of photosynthate
623 away from leaves and out to roots is lower in the HS than in the LS treatment. One

624 possible interpretation is that the rate of flow within a given phloem pathway is relatively
625 constant, and that more phloem pathways towards the roots are active when production of
626 photosynthate is high. A logical consequence of that arrangement would be that at any
627 given point along the transport pathway towards the roots, or at any point in time at a
628 given location along the pathway, the concentration of a common-sized label would be
629 lower for a tree with high rate of ongoing photosynthesis than for a tree with low rate of
630 ongoing photosynthesis, due to dilution of the fixed-size label into a larger number
631 (larger cross-sectional area) of transport pathways, all with a common transport velocity
632 (conceptual model shown in Fig. 7). This is in fact the observed relationship of LS to HS
633 concentration at all points in time for both the phloem measurements (fixed point on the
634 trunk) and for the soil surface CO_2, lending support to the hypothesized mechanism.
635 Plant storage pools in the form of non-structural carbohydrates are known to play
636 an important role in regulating allocation to structural pools, and may make up a
637 significant portion of total biomass (e.g. Hoch et al., 2003). Simple models that account
638 for non-structural carbohydrates better compare with observed ^{14}C and stem growth,
639 indicating the importance of the pools over seasonal to decadal timescales (Richardson et
640 al., 2013). The question remains: What are the consequences for a CLM like model of
641 ignoring the shorter timescale (monthly) storage dynamics? (see Fig. 7). If we show that
642 the modeled and observed label concentrations tend to converge over monthly timescales,
643 we can argue that ignoring these short-term pools is not a first-order impediment to good
644 estimates of allocation and growth. Other more subtle aspects of the problem could,
645 however, have important implications for plot-scale and even global scale vegetation-soil
646 ecosystem dynamics and feedbacks. For example, the labeled soil surface CO_2 efflux is a

result from a combination of root respiration and heterotrophic respiration. The heterotrophic component can be supplied by fresh litter inputs or by root exudation of non-structural carbohydrate, which can be a significant fraction of net primary production in some systems (Högberg et al., 2010). The difference between root mortality and root exudation in terms of substrate quality, nutrient content, and interactions with soil microbial communities could be very significant, especially as integrated over long periods and under conditions of changing climate, changing atmospheric CO_2 concentration, and anthropogenic modifications to nutrient cycles.

Representing the existence and dynamics of short-term photosynthate storage pools in a model like CLM could also help to resolve the mechanisms relating nutrient mineralization and availability in soils with plant-microbe competition for available nutrients and the influence of nutrient uptake on leaf-scale photosynthesis. In addition to the shading treatments described here, other manipulations that would be useful to explore include elevated CO_2 during and/or after the labeling pulse, imposed nutrient limitations, and fertilization. Replicating these studies in other vegetation types would help to assess the generality of storage pool structure and function, and would support operational inclusion of these mechanisms in a global-scale model.

4.3 Implications for experimental design

Limitations identified in this first PiTS model-experiment interaction have already led to improvements in follow-on experiments. For new experiments in a nearby dogwood stand, additional observations include multiple treatments in different seasons, a collection of absolute destructive tree biomass at the end of the study (rather than highly uncertain estimates based on allometric relationships), seasonal leaf-level photosynthetic

measurements, assessment of mycorrhizal C flux, and improved meteorological measurements. Although model parameters can be improved through optimization as in this study, model parameters are being measured where possible. These additional observational data are necessary for more detailed model evaluation and improvement of model routines of C and allocation patterns at various time scales. Additional effort is being devoted to characterizing the system prior to manipulation, including measurements of biomass, soil physical and soil biogeochemical states.

5 Conclusions

The point version of CLM4 was implemented, calibrated and evaluated against carbon and hydrology observations from a shading and labeling experiment in a stand of young loblolly pines. We found that a combination of parameters measured on-site and calibration targeting biomass, transpiration, and ^{13}C discrimination gave good agreement with pretreatment measurements, including independent evaluation metrics at the leaf-scale. We showed that the calibrated model captured the tree-scale and monthly temporal dynamics of a light-shade treatment as it influenced carbon and water fluxes. The calibrated model also captured the monthly time-scale carbon dynamics of a heavy-shade treatment, but persistently estimated low levels of transpiration for the heavy-shade treatment, while observed transpiration in that treatment remained nearly as high as for the light-shade. We have suggested several possible explanations for the discrepancy, but this remains a puzzling problem requiring further investigation.

Although the model lacks short-term photosynthate storage and transport mechanisms that are clearly present in the real plants, first-order monthly time-scale

693 dynamics for carbon allocation and growth do not seem to suffer greatly. We used
694 observations from the experiment to develop a conceptual model (hypothesis) of short-
695 term photosynthate storage and transport, and suggested further studies that could be
696 carried out to evaluate the generality of the hypothesized mechanisms. We suggest
697 several research problems, which, if the proposed mechanism turns out to be generally
698 valid, would benefit from model-experimental study in which the new mechanisms are
699 incorporated into the model structure.
700
701 *Acknowledgements.* This work is supported by the US Department of Energy (DOE),
702 Office of Science, Biological and Environmental Research. Oak Ridge National
703 Laboratory is managed by UT-BATTELLE for DOE under contract DE-AC05-
704 00OR22725.
705

706 ## References

707 Amthor, J. S., Chen, J. M., Clein, J. S., Frolking, S. E., Goulden, M. L., Grant, R. F.,
708 Kimball, J. S., King, A. W., McGuire, A. D., Nikolov, N. T., Potter, C. S., Wang, S.,
709 and Wofsy, S. C.: Boreal forest CO_2 exchange and evapotranspiration predicted by
710 nine ecosystem process models: Intermodel comparisons and relationships to field
711 measurements, J. Geophys. Res.-Atmos., 106, 33623-33648, 2001.
712 Arora, V. K., Boer, G. J., Friedlingstein, P., Eby, M., Jones, C. D., Christian, J. R.,
713 Bonan, G., Bopp, L., Brovkin, V., and Cadule P.: Carbon–concentration and carbon–
714 climate feedbacks in CMIP5 Earth system models, J. Climate, 26, 5289-5314, 2013.

715 Atkin, O.: New phytologist and the ‘fate’ of carbon in terrestrial ecosystem, New Phytol,
716 205,1-3, 2015.
717 Badeck, F. W., Tcherkez, G., Nogues, S., Piel, C., and Ghashghaie, J.: Post-photo
718 synthetic fractionation of stable carbon isotopes between plant organs - a widespread
719 phenomenon, Rapid Commun Mass Sp, 19(11), 1381-1391, 2005.
720 Bahn, M., Buchmann, N., and Knohl, A.: Preface "Stable Isotopes and Biogeochemical
721 Cycles in Terrestrial Ecosystems", Biogeosciences, 9, 3979-3981, 2012.
722 Baldocchi, D., Falge, E., Gu, L., Olson, R., Hollinger, D., Running, S., Anthoni, P.,
723 Bernhofer, C., Davis, K., and Evans R.: FLUXNET: A new tool to study the temporal
724 and spatial variability of ecosystem-scale carbon dioxide, water vapor, and energy flux
725 densities, B. Am. Meteorol. Soc., 82, 2415-2434, 2001.
726 Baldwin, V. C. and Feduccia, D. P.: Loblolly pine growth and yield prediction for
727 managed west Gulf plantations, USDA For. Ser. Res. Pap., SO-236, New Orleans, LA:
728 U.S. Department of Agriculture, Forest Service, Southern Forest Experiment Station,
729 27 pp., 1987.
730 Barnard, D. M., and Bauerle, W. L.: The implications of minimum stomatal conductance
731 on modeling water flux in forest canopies, J. Geophys. Res.-Biogeo., 118, 1322-1333,
732 2013.
733 Bauerle, W. L., Oren, R., Way, D. A., Qian, S. S., Stoy, P. C., Thornton, P. E., Bowden,
734 J. D., Hoffman, F. M., and Reynolds, R. F.:, Photoperiodic regulation of the seasonal
735 pattern of photosynthetic capacity and the implications for carbon cycling, P. Natl.
736 Acad. Sci. USA, 109, 8612-8617, 2012.

737 Beer, C., Reichstein, M., Tomerlleri, E., Ciais, P., Jung, M., Carvalhai, N., Rodenbeck,
738 C., Arain, M. A., Baldocchi, D., Bonan, G. B., Bondeau, A., Cescatti, A., Lasslop, G.,
739 Lindroth, A., Lomas, M., Luyssaert, S., Margolis, H., Oleson, K. W., Roupsard, O.,
740 Veenendaal, E., Viovy, N., Williams, C., Woodward, F. I., and Papale, D.: Terrestrial
741 gross carbon dioxide uptake: global distribution and covariation with climate, Science,
742 329, 834-838, 2010.
743 Best, M. J., Pryor, M., Clark, D. B., Rooney, G. G., Essery, R. L. H., Menard, C. B.,
744 Edwards, J. M., Hendry, M. A., Porson, A., Gedney, N., Mercado, L. M. Sitch, S.,
745 Blyth, E., Boucher, O., Cox, P. M., Grimmond, C. S. B., and Harding, R. J.: The Joint
746 UK Land Environment Simulator (JULES), model description - Part 1: Energy and
747 water fluxes, Geosci. Model Dev., 4, 677-699, 2011.
748 Bonan, G. B., Hartman, M. D., Parton, W. J., and Wieder, W. R.: Evaluating litter
749 decomposition in earth system models with long-term litterbag experiments: an
750 example using the Community Land Model version 4 (CLM4), Glob. Change Biol.,
751 19, 957-974, 2013.
752 Bonan, G. B., Lawrence, P. J., Oleson, K. W., Levis, S., Jung, M., Reichstein, M.,
753 Lawrence, D. M., and Swenson, S. C.: Improving canopy processes in the Community
754 Land Model version 4 (CLM4) using global flux fields empirically inferred from
755 FLUXNET data, J. Geophys. Res.-Biogeo., 116 ,2011.
756 Bonan, G. B., Oleson, K. W., Fisher, R. A., Lasslop, G., and Reichstein, M.: Reconciling
757 leaf physiological traits and canopy flux data: Use of the TRY and FLUXNET
758 databases in the Community Land Model version 4, J. Geophys. Res.-Biogeo., 117,
759 2012.

760 Cannell, M. G. R. and Dewar R. C.: Carbon allocation in trees - a review of concepts for
761 modeling, Adv. Ecol. Res., 25, 59-104, 1994.
762 Dai, Y. J., Zeng, X. B., Dickinson, R. E., Baker, I., Bonan, G. B., Bosilovich, M. G.,
763 Denning, A. S., Dimeyer, P. A., Houser, P. A., Niu, G. Y., Oleson, K. W., Scholosser,
764 C. A., and Yang, Z., L.: The common land model, B. Am. Meteorol. Soc., 84, 1013-+,
765 doi: 10.1175/BAMS-84-8-1013, 2003.
766 Damour, G., Simonneau, T., Cochard, H., and Urban, L.: An overview of models of
767 stomatal conductance at the leaf level, Plant Cell Environ., 33, 1419-1438, 2010.
768 De Kauwe, M. G., Medlyn, B. E., Zaehle, S., Walker, A. P., Dietze, M. C., Hickler, T.,
769 Jain, A. K., Luo, Y. Q., Parton, W. J., Prentice, I. C., Smith, B., Thornton, P. E.,
770 Wang, S. S., Wang, Y. P., Warlind, D., Weng, E. S., Crous, K. Y., Ellsworth, D. S.,
771 Hanson, P. J., Seok Kim, H., Warren, J. M., Oren, R., and Norby R. J.,: Forest water
772 use and water use efficiency at elevated CO_2: a model-data intercomparison at two
773 contrasting temperate forest FACE sites, Glob. Change Biol., 19, 1759-1779, 2013.
774 De Kauwe, M. G., Medlyn, B. E., Zaehle, S., Walker, A. P., Dietze, M. C., Wang, Y. P.,
775 Luo, Y. Q., Jain, A. K., El-Masri, B., Hickler, T., Warlind, D., Weng, E. S., Parton, W.
776 J., Thornton, P. E., Wang, S. S., Prentice, I. C., Asao, S., Smith, B., McCarthy, H. R.,
777 Iversen, C. M., Hanson, P. J., Warren, J. M., Oren, R., and Norby, R. J.: Where does
778 the carbon go? A model–data intercomparison of vegetation carbon allocation and
779 turnover processes at two temperate forest free-air CO_2 enrichment sites, New Phytol.,
780 203, 883-899, 2014.
781 Domec J.C., Ogée J, Noormets A., Jouangy J. Gavazzi M., Treasure E., Sun G., McNulty
782 S. and J.S. King. 2012. Interactive effects of nocturnal transpiration and climate

783 change on the root hydraulic redistribution and carbon and water budgets of Southern
784 US pine plantations. Tree Physiology 32(6): 707-723.
785 Ehleringer, J. R., Buchmann, N., and Flanagan, L. B.: Carbon isotope ratios in
786 belowground carbon cycle processes, Ecological Applications, 10, 412-422, 2000.
787 Epron, D., Bahn, M., Derrien, D., Lattanzi, F. A., Pumpanen, J., Gessler, A., Hogberg, P.,
788 Maillard, P., Dannoura, M., Gerant, D., and Buchmann, N.: Pulse-labelling trees to
789 study carbon allocation dynamics: a review of methods, current knowledge and future
790 prospects, Tree Physiol., 32, 776-798, 2012.
791 Farquhar, G. D., J. R. Ehleringer, and K. T. Hubick: Carbon Isotope Discrimination and
792 Photosynthesis, Annu Rev Plant Phys, 40, 503-537, 1989.
793 Fox, A., Williams, M., Richardson, A. D., Cameron, D., Gove, J. H., Quaife, T., Ricciuto,
794 D., Reichstein, M., Tomelleri, E., Trudinger, C. M., and Van Wijk, M. T.: The
795 REFLEX project: Comparing different algorithms and implementations for the
796 inversion of a terrestrial ecosystem model against eddy covariance data, Agr. Forest
797 Meteorol., 149, 1597-1615, 2009.
798 Friedlingstein, P., Cox, P., Betts, R., Bopp, L., Von Bloh, W., Brovkin, V., Cadule, P.,
799 Doney, S., Eby, M., Fung, I., Bala, G., John, J., Jones, C., Joos, F., Kato, T.,
800 Kawamiya, M., Knorr, W., Lindsay, K., Matthews, H. D., Raddatz, T., Rayner, P.,
801 Reick, C., Roeckner, E., Schnitzler, K. G., Schnur, R., Strassmann, K., Weaver, A. J.,
802 Yoshikawa, C., and Zeng, N.: Climate-carbon cycle feedback analysis: Results from
803 the (CMIP)-M-4 model intercomparison, J. Climate, 19, 3337-3353, 2006.
804 Gent, P. R., Danabasoglu, G., Donner L. J., Holland, M. M., Hunke, E. C., Jayne, S. R.,
805 Lawrence, K. M., Neale, R. B., Rasch, P. J., Vertenstein, M., Worley P. H., Yang Z. L,

806 and Zhang, M. H.: The Community Climate System Model Version 4, J. Climate, 24,
807 4973-4991, 2011.
808 Griffin, K. L., Winner, W. E., and Strain, B. R.: Growth and dry matter partitioning in
809 loblolly and ponderosa pine seedlings in response to carbon and nitrogen availability,
810 New Phytol., 129, 547-556, 1995.
811 Hamilton, J. G., Thomas, R. B., and Delucia, E. H.: Direct and indirect effects of elevated
812 CO2 on leaf respiration in a forest ecosystem, Plant Cell Environ., 24, 975-982, 2001.
813 Hanson, P. J., Amthor, J. S., Wullschleger, S. D., Wilson, K. B., Grant, R. F., Hartley, A.,
814 Hui, D., Hunt, E. R., Johnson, D. W., Kimball, J. S., King, A. W., Luo, Y., McNulty,
815 S. G., Sun, G., Thornton, P. E., Wang, S., Williams, M. Baldocchi, D. D., and
816 Cushman, R. M.: Oak forest carbon and water simulations: Model intercomparisons
817 and evaluations against independent data, Ecol Monogr., 74, 443-489. 2004.
818 Hoch, G., Richter, A., and Korner, C.: Non-structural carbon compounds in temperate
819 forest trees, Plant Cell Environ, 26(7), 1067-1081, 2003.
820 Högberg, M. N., Briones, M. J. I., Keel, S. G., Metcalfe, D. B., Campbell, C., Midwood,
821 A. J., Thornton, B., Hurry, V., Linder, S., Näsholm, T., and Högberg, P.:
822 Quantification of effects of season and nitrogen supply on tree below-ground carbon
823 transfer to ectomycorrhizal fungi and other soil organisms in a boreal pine forest. *New*
824 *Phytol.* 187, 485-493, 2010.
825 Huntzinger, D. N., Post, W. M., Wei, Y., Michalak, A. M., West, T. O., Jacobson, A. R.,
826 Baker, I. T., Chen, J. M, Davis, K. J., Hayes, D. J., Hoffman, F. M., Jain, A. K., Liu,
827 S., McGuire, A. D., Neilson, R. P., Potter, C., Poulter, B., Price, D., Raczka, B. M.,
828 Tian, H. Q., Thornton, P. E., Tomelleri, E., Viovy, N., Xiao, J., Yuan, W., Zeng, N.,

829 Zhao, M., and Cook, R.: North American Carbon Program (NACP) regional interim
830 synthesis: Terrestrial biospheric model intercomparison, Ecol. Model., 232, 144-157,
831 2012.
832 Idso, S. B.: A set of equations for full spectrum and 8-mu-m to 14-mu-m and 10.5-mu-m
833 to 12.5-mu-m thermal-radiation from cloudless skies, Water Resour. Res., 17., 295-
834 304, 1981.
835 Keenan, T. F., Carbone, M. S., Reichstein, M., and Richardson, A. D.: The model-data
836 fusion pitfall: assuming certainty in an uncertain world, Oecologia, 167, 587-597,
837 2011.
838 Koven, C. D., Riley, W. J., Subin, Z. M., Tang, J. Y., Torn, M. S., Collins, W. D., Bonan,
839 G. B., Lawrence, D. M., and Swenson S. C.: The effect of vertically resolved soil
840 biogeochemistry and alternate soil C and N models on C dynamics of CLM4,
841 Biogeosciences, 10, 7109-7131, 2013.
842 Krinner, G., Viovy, N., de Noblet-Ducoudre, N., Ogee, J., Polcher, J., Friedlingstein, P.,
843 Ciais, P., Sitch, S., and Prentice, I. C.: A dynamic global vegetation model for studies
844 of the coupled atmosphere-biosphere system, Global Biogeochem. Cy., 19, 2005.
845 Lawrence, D. M., Oleson, K. W., Fanner, M. G., Thornton, P. E., Swenson, S. C.,
846 Lawrence, P. J., Zeng, X. B., Yang, Z. L., Levis, S., Sakaguchi, K., Bonan, G. B., and
847 Slater, A. G.: Parameterization improvements and functional and structural advances
848 in version 4 of the Community Land Model, J. Adv. Model Earth Sy., 3., M03001,
849 2011.
850 Li, H. Y., Huang, M. Y., Wigmosta, M. S., Ke, Y. H., Coleman, A. M., Leung, L. R.,
851 Wang, A. H., and Ricciuto, D. M.: Evaluating runoff simulations from the Community

852 Land Model 4.0 using observations from flux towers and a mountainous watershed, J.
853 Geophys. Res.-Atmos., 116, 2011.
854 Litton, C. M., Raich, J. W., and Ryan, M. G.: Carbon allocation in forest ecosystems,
855 Glob. Change Biol., 13, 2089-2109, 2007.
856 Luo, Y. Q., Randerson, J. T., Abramowitz, G., Bacour, C., Blyth, E., Carvalhais, N.,
857 Ciais, P., Dalmonech, D., Fisher, J. B., Fisher, R., Friedlingstein, P., Hibbard, K.,
858 Hoffman, F., Hunzinger, D., Jones, D. D., Koven, C., Lawrence, D., Li, D. J.,
859 Mahecha, M., Niu, S. L., Norby, R., Piao, S. L., Qi, X., Peylin, P., Prentice, I. C.,
860 Riley, W., Reichstein, M., Schwalm, C., Wang, Y. P., Xia, J. Y., Zaehle, S., and Zhou,
861 X. H.: A framework for benchmarking land models, Biogeosciences, 9, 3857-3874,
862 2012.
863 Mao, J. F., Shi, X. Y., Thornton, P. E., Piao, S. L., and Wang, X. H.: Causes of spring
864 vegetation growth trends in the northern mid-high latitudes from 1982 to 2004,
865 Environ. Res. Lett., 7, 014010, 2012a.
866 Mao, J. F., Thornton, P. E., Shi, X. Y., Zhao, M. S., and Post, W. M.: Remote sensing
867 evaluation of CLM4 GPP for the period 2000-09, J. Climate, 25, 5327-5342, 2012b.
868 Mao, J. F., Shi, X. Y., Thornton, P. E., Hoffman, F. M., Zhu, Z. C., and Myneni, R. B.:
869 Global latitudinal-asymmetric vegetation growth trends and their driving mechanisms:
870 1982-2009, Remote Sens.-Basel, 5, 1484-1497, 2013.
871 Naidu, S. L., DeLucia, E. H., and Thomas, R. B.: Contrasting patterns of biomass
872 allocation in dominant and suppressed loblolly pine, Can. J. Forest Res., 28, 1116-
873 1124, 1998.

874 Oleson, K., Lawrence, D. M., Bonan, G. B., Drewniak, B., Huang, M., Koven, C. D.,
875 Levis, S., Li, F., Riley, W. J., Subin, Z. M., Swenson, S., Thornton, P. E., Bozbiyik,
876 A., Fisher R.,. Heald, C. L, Kluzek, E., Lamarque, J. -F., Lawrence, P. J., Leung, L. R.,
877 Lipscomb, W., Muszala, S. P., Ricciuto, D. M., Sacks, W. J., Sun, Y., Tang, J., and
878 Yang, Z. -L.: Technical description of version 4.5 of the Community Land Model
879 (CLM), NCAR Technical Note NCAR/TN-503+STR, The National Center for
880 Atmospheric Research (NCAR): Boulder, CO, USA,420 pp., 2013.
881 Oleson, K. W., Lawrence, D. M., Gordon, B., Flanner, M. G., Kluzek, E., Lawrence, P.,
882 J., Levis, S., Swenson, S. C., Thornton, P. E., Dai, A., Decker, M., Dickinson, R.,
883 Feddema, J., Heald, C. L., Hoffman, F., Lamarque, J. –F., Mahowald, N., Niu, G. –Y.,
884 Qian, T., Randerson, J., Running, S., Sakaguchi, K., Slater, A., Stoeckli, R., Wang, A,
885 Yang, Z. –L., Zeng, X. D., and Zeng, X. B.: Technical description of version 4.0 of the
886 Community Land Model (CLM), NCAR Technical Note NCAR/TN 478+STR; The
887 National Center for Atmospheric Research (NCAR): Boulder, CO, USA, 257 pp.,
888 2010.
889 Oleson, K. W., Niu, G. –Y., Yang, Z. –L., Lawrence, D. M., Thornton, P. E., Lawrence,
890 P. J., Stoeckli, R., Dickinson, R. E., Bonan, G. B., Levis, S., Dai, A., and Qian, T.:
891 Improvements to the Community Land Model and their impact on the hydrological
892 cycle, J. Geophys. Res.-Biogeo., 113, G01021, 2008.
893 Ostle, N. J., Smith, P., Fisher, R., Woodward, F. I., Fisher, J. B., Smith, J. U., Galbraith,
894 D., Levy, P., Meir, P., McNamar, N. P., and Bardgett, R. D.: Integrating plant-soil
895 interactions into global carbon cycle models, J. Ecol., 97, 851-863, 2009.

Pitman, A. J.: The evolution of, and revolution in, land surface schemes designed for climate models, Int. J. Climatol., 23, 479-510, 2003.

Raczka, B. M., Davis, K. J., Huntzinger, D., Neilson, R. P., Poulter, B., Richardson, A. D., Xiao, J. F., Baker, I., Ciais, P., Keenan, T. F., Law, B., Post, W. M., Ricciuto, D., Schaefer, K., Tian, H. Q., Tomelleri, E., Verbeeck, H., and Viovy, N.:. Evaluation of continental carbon cycle simulations with North American flux tower observations, Ecol. Monogr., 83., 531-556, 2013.

Randerson, J. T., Hoffman, F. M., Thornton, P. E., Mahowald, N. M., Lindsay, K., Lee, Y. H., Nevison, C. D., Doney, S. C., Bonan, G., Stoeckli, R., Covey, C., Running, S. W., and Fung, I. Y.: Systematic assessment of terrestrial biogeochemistry in coupled climate-carbon models, Glob. Change Biol., 15 2462-2484, 2009.

Ricciuto, D. M., King, A. W., Dragoni, D., and Post, W. M.: Parameter and prediction uncertainty in an optimized terrestrial carbon cycle model: Effects of constraining variables and data record length, J. Geophys. Res.-Biogeo., 116, 2011.

Richardson, A. D., Carbone, M. S., Keenan, T. F., Czimczik, C. I., Hollinger, D. Y., Murakami, P., Schaberg, P. G., and Xu X. M.: Seasonal dynamics and age of stemwood nonstructural carbohydrates in temperate forest trees, New Phytol, 197(3), 850-861, 2013.

Richardson, A. D., Anderson, R. S., Arain, M. A., Barr, A. G., Bohrer, G., Chen, G. S., Chen, J. M., Ciais, P., Davis, K. J., Desai, A. R., Dietze, M. C., Dragoni, D., Garrity, S. R., Gough, C. M., Grant, R., Hollinger, D. Y., Margolis, H. A., McCaughey, H., Migliavacca, M., Monson, R. K., Munger, J. W., Poulter, B., Raczka, B. M., Ricciuto, D. M., Sahoo, A. K., Schaefer, K., Tian, H. Q., Vargas, R., Verbeeck, H., Xiao, J. F.,

and Xue, Y. K.: Terrestrial biosphere models need better representation of vegetation phenology: results from the North American Carbon Program Site Synthesis, Glob. Change Biol., 18, 566-584, 2012.

Richardson, A. D., Williams, M., Hollinger, D., Moore, D., Dail, D., Davidson, E., Scott, N., Evans, R., Hughes, H., Lee, J., Ro- drigues, C., and Savage, K.: Estimating parameters of a forest ecosystem C model with measurements of stocks and fluxes as joint constraints, Oecologia, 164, 25–40, 2010.

Riley, W. J., Subin, Z. M., Lawrence, D. M., Swenson, S. C., Torn, M. S., Meng, L., Mahowald, N. M., and Hess, P.: Barriers to predicting changes in global terrestrial methane fluxes: analyses using CLM4Me, a methane biogeochemistry model integrated in CESM, Biogeosciences, 8, 1925-1953, 2011.

Runarsson, T. P., and Yao X.: Stochastic ranking for constrained evolutionary optimization, IEEE T. Evolut. Comput., 4., 284-294, 2000.

Sargsyan, K., Safta, C., Habib, N. N., Debusschere, B. J., Ricciuto, D., and Thornton, P. E.: Dimensionality reduction for complex models via bayesian compressive sensing, Int. J. Uncertain. Quant., 4, 63-93, 2013.

Schaefer, K., Schwalm, C. R., Williams, C., Arain, M. A., Barr, A., Chen, J. M., Davis, K. J., Dimitrov, D., Hilton, T. W., Hollinger, D. Y., Humphreys, E., Poulter, B., Raczka, B. M., Richardson, A. D., Sahoo, A., Thornton, P. E., Vargas, R., Verbeeck, H., Anderson, R., Baker, I., Black T. A., Bolstad, P., Chen, J. Q., Curtis, P. S., Desai, A. R., Dietze, M., Dragoni, D., Gough, C., Grant, R. F., Gu, L. H., Jain, A., Kucharik, C., Law, B., Liu, S. G., Lokipitiya, E., Margolis, H. A., Matamala, R., McCaughey, J. H., Monson, R., Munger, J. W., Oechel, W., Peng, C. H., Price, D. T., Ricciuto, D.,

942 Riley, W. J., Roulet, N., Tian, H. Q. Tonitto, C., Torn, M., Weng, e. S., and Zhou, X.
943 L.: A model-data comparison of gross primary productivity: Results from the North
944 American Carbon Program site synthesis, J. Geophys. Res.-Biogeo., 117, 2012.
945 Schimel, D. S., House, J. I., Hibbard, K. A., Bousquet, P., Ciais, P., Peylin, P., Braswell,
946 B. H., Apps, M. J., Baker, D., Bondeau, A., Canadell, J., Churkina, G., Cramer, W.,
947 Denning, A. S., Field, C. B. Friendlingstein, P., Goodale, C., Heimann, M., Houghton,
948 R. A., Melillo, J. M., Moore, B., Murdiyarso, D., Noble, I., Pacala, S. W., Prentice, I.
949 C., Raupach, M. R., Rayner, P. J., Scholes, R. J., Steffen, W. L., and Wirth, C.: Recent
950 patterns and mechanisms of carbon exchange by terrestrial ecosystems, Nature, 414,
951 169-172, 2001.
952 Schwalm, C. R., Williams, C. A., Schaefer, K., Anderson, R., Arain, M. A., Baker, I.,
953 Barr, A., Black, T. A., Chen, G. S., Chen, J. M., Ciais, P., Davis, K. J., Desai, A.,
954 Dietze, M., Dragoni, D., Fischer, M. L., Flanagan, L. B., Grant, R., Gu, L. H.,
955 Hollinger, D., Izaurralde, R. C., Kucharik, C., Lafleur, P., Law, B. E., Li, L. H., Li, Z.
956 P., Liu, S. G., Lokupitiya, E., Luo, Y. Q., Ma, S. Y., Margolis, H., Matamala, R.,
957 McCaughey, H., Monson, R. K., Oechel, W. C., Peng, C. H., Poulter, B., Price, D. T.,
958 Ricciuto, D. M., Riley, W., Sahoo, A. K., Sprintsin, M., Sun, J. F., Tian, H. Q.,
959 Tonitto, C., Verbeeck, H. and Verma, S. B.: A model-data intercomparison of CO_2
960 exchange across North America: Results from the North American Carbon Program
961 site synthesis, J. Geophys. Res.-Biogeo., 115, 2010.
962 Shi, X., Mao, J., Thornton, P. E., Hoffman, F. M., and Post, W. M.: The impact of
963 climate, CO_2, nitrogen deposition and land use change on simulated contemporary
964 global river flow, Geophys. Res. Lett., 38, L08704, 2011.

965 Shi, X. Y., Mao, J. F., Thornton, P. E., and Huang, M. Y.: Spatiotemporal patterns of
966 evapotranspiration in response to multiple environmental factors simulated by the
967 Community Land Model, Environ. Res. Lett., 8, 024012, 2013.
968 Shi, X. Y., Thornton, P. E., Ricciuto, D. M., Hanson, P. J., Mao, J. F., Sebestyen, S. D.,
969 Griffiths, N. A., and Bisht G.: Representing northern peatland microtopography and
970 hydrology within the Community Land Model, Biogeosciences, 12, 6463-6477, doi:
971 10.5194/bg-12-6463-2015, 2015.
972 Stoy, P. C., Dietze, M. C., Richardson, A. D., Vargas, R., Barr, A. G., Anderson, R. S.,
973 Arain, M. A., Baker, I. T., Black T. A., Chan, J. M., Cook, R. B., Gough, C. M., Grant,
974 R. F., Hollinger, D. Y., Izaurralde, R. C., Kucharik, C. J., Lafleur, P., Law, B. E., Liu,
975 S., Lokupitiya, E., Luo, Y., Munger, J. W., Peng, C., Poulter, B., Price, D. T.,
976 Ricciuto, D. M., Riley, W. J., Sahoo, A. K., Schaefer, K., Schwalm, C. R., Tian, H.,
977 Verbeeck, H., and Weng, E.: Evaluating the agreement between measurements and
978 models of net ecosystem exchange at different times and timescales using wavelet
979 coherence: an example using data from the North American Carbon Program Site-
980 Level Interim Synthesis, Biogeosciences, 10, 6893-6909, 2013.
981 Taylor, K. E., Stouffer, R. J., and Meehl, G. A.: An Overview of CMIP5 and the
982 Experiment Design, B. Am. Meteorol. Soc., 93, 485-498, 2012.
983 Tissue, D. T., Thomas, R. B., and Strain, B. R.: Growth and photosynthesis of loblolly
984 pine (*Pinus taeda*) after exposure to elevated CO_2 for 19 months in the field, Tree
985 Physiol., 16, 49-59,1995.

986 Thornton, P. E., and Rosenbloom, N. A.: Ecosystem model spin-up: Estimating steady
987 state conditions in a coupled terrestrial carbon and nitrogen cycle model, Ecol. Model.,
988 189, 25-48, 2005.
989 Thornton, P. E., Lamarque, J. F., Rosenbloom, N. A., and Mahowald, N. M.: Influence of
990 carbon-nitrogen cycle coupling on land model response to CO_2 fertilization and
991 climate variability, Global Biogeochem. Cy., 21, 2007.
992 Vandegehuchte, M. W., Guyot, A., Hubeau, M., De Swaef, T., Lockington, D. A., and
993 Steppe, K.: Modelling reveals endogenous osmotic adaptation of storage tissue water
994 potential as an important driver determining different stem diameter variation patterns
995 in the mangrove species *Avicennia marina* and Rhizophora stylosa, Ann. Bot., 114,
996 667-676, doi:10.1093/aob/mct311, 2014.
997 Vanlear, D. H., Taras, M. A., Waide, J. B., and Augspurger, M. K.: Comparison of
998 biomass equations for planted vs. natural loblolly-pine stands of sawtimber size, Forest
999 Ecol. Manag., 14, 205-210, 1986.
1000 Walker, A. P., Hanson, P. J.., De Kauwe, M. G., Medlyn,B. E., Zaehle, S., Asao, S.,
1001 Dietze, M., Hickler, T., Huntingford, C., Iversen C. M., Jain, A., Lomas, M., Luo Y.,
1002 McCarthy, H., Parton, W. J., Prentice, I. C.., Thornton, P. E., Wang S., Wang, Y. –P.,
1003 Warlind, D., Weng, E., Warren, J. M., Woodward, F. I., Oren, R., and Norby, R. J.:
1004 Comprehensive ecosystem model-data synthesis using multiple data sets at two
1005 temperate forest free-air CO_2 enrichment experiments: Model performance at ambient
1006 CO_2 concentration, J. Geophys. Res. Biogeosci., 119, 937-964, 2014.

1007 Wang, D. L., Xu, Y., Thornton, P. E., King, A., Steed, C., Gu, L. H., and Schuchart, J.: A
1008 functional test platform for the Community Land Model, Environ. Modell. Softw., 55,
1009 25-31, 2014.
1010 Wang, Y. P., Kowalczyk, E., Leuning, R., Abramowitz, G., Raupach, M. R., Pak, B., van
1011 Gorsel, E., and Luhar, A.: Diagnosing errors in a land surface model (CABLE) in the
1012 time and frequency domains, J. Geophys. Res.-Biogeo., 116, 2011.
1013 Warren, J. M., Norby, R. J., and Wullschleger, S. D.: Elevated CO_2 enhances leaf
1014 senescence during extreme drought in a temperate forest, Tree Physiol., 31, 117-130,
1015 2011.
1016 Warren, J. M., Iversen, C. M., Garten, C. T., Norby, R. J., Childs, J., Brice, D., Evans, R.
1017 M., Gu, L., Thornton, P. E., and Weston, D. J.: Timing and magnitude of C
1018 partitioning through a young loblolly pine (Pinus taeda L.) stand using C-13 labeling
1019 and shade treatments, Tree Physiol., 32, 799-813, 2012.
1020 Warren, J. M., Iversen, C. M., Garten Jr., C. T., Norby, R. J., Childs, J., Brice, D., Evans,
1021 R. M., Gu, L., Thornton, P. E., and Weston, D. J.: PiTS-1: Carbon partitioning in
1022 loblolly pine after ^{13}C labeling and shade treatments, Carbon Dioxide Information
1023 Analysis Center, Oak Ridge National Laboratory, U.S. Department of Energy, Oak
1024 Ridge, Tennessee, U.S.A., doi: 10.3334/CDIAC/ornlsfa.001, 2013.
1025 White, M. A., Thornton P. E., Running S. W., and Nemani R. R.: Parameterization and
1026 sensitivity analysis of the BIOME-BGC terrestrial ecosystem model: net primary
1027 production controls, Earth Interactions, 4, 1–85, 2000.
1028 Williams, M., Richardson, A. D., Reichstein, M., Stoy, P. C., Peylin, P., Verbeeck, H.,
1029 Carvalhais, N., Jung, M., Hollinger, D. Y., Kattge, J., Leuning, R., Luo, Y., Tomelleri,

E., Trudinger, C. M., and Wang, Y. –P.: Improving land surface models with FLUXNET data, Biogeosciences, 6, 1341-1359, 2009.

Wullschleger, S. D., Hanson, P. J., and Todd, D. E.:Transpiration from a multi-species deciduous forest as estimated by xylem sap flow techniques, Forest Ecol. Manag., 143, 205-213, 2001.

Zaehle, S., Medlyn, B. E., De Kauwe, M. G., Walker, A. P., Dietze, M. C., Hickler, T., Luo, Y. Q., Wang, Y. P., El-Masri, B., Thornton, P., Jain, A., Wang, S. S., Warlind, D., Weng, W. S., Parton, W., Iversen, C. M., Gallet-Budynek, A., McCarthy, H., Finzi, A. C., Hanson, P. J., Prentice, I. C., Oren, R. and Norby, R. J.: Evaluation of 11 terrestrial carbon-nitrogen cycle models against observations from two temperate Free-Air CO_2 Enrichment studies, New Phytol., 202, 803-822, 2014.

Table 1.

Parameter	Description	Units	Default	Observed	PRE_OPT	HS_MB
measured						
slatop	Top of canopy specific leaf area (SLA)	m^2/gC	1.00E-02	1.02E-02	none	1.02E-02
dsladlai	Change in SLA through per unit LAI	gC^{-1}	1.25E-03	0	none	0
leafcn	leaf C:N ratio	gC/gN	35	50	none	50
optimized						
mp	Ball-Berry stomatal conductance slope	none	6	none	5.59	71.3
bp	Ball-Berry stomatal conductance intercept	$\mu mol\ m^{-2}\ s^{-1}$	5000	none	4960	61100
froot_leaf	fine root to leaf allocation ratio	none	1	none	1.24	1.24
stem_leaf	stem to leaf allocation ratio	none	2.2*	none	3.29	3.29
flnr	fraction of leaf N in RuBisCO	none	0.05	none	0.0845	0.0845
q10_mr	maintenance respiration t-sensitivity	none	1.5	none	2.83	2.83

*** stem-leaf allocation is a function of annual NPP. 2.2 is the nominal value at NPP = 800 gC m^{-2} yr^{-1}**

Table 2.

State variable	Units	Observed	PRE_STD	PRE_OPT	Bias reduction (%)
Leaf carbon	gC/m^2	[182,221]	419	209	96.55
Stem carbon	gC/m^2	[973,1220]	1455	1027	88.49
Root carbon	gC/m^2	488	859	408	78.44
Aboveground biomass	gC/m^3	[728,1758]	1645	1236	98.26
δ13C leaf	per mil	-27.99	-27.38	-27.49	18.03
δ13C phloem	per mil	-28.48	-27.38	-27.50	10.91
δ13C Root	per mil	-28.86	-27.36	-27.39	2.13
Sap flow	mm/day	2.40	3.70	2.37	97.85
Soil respiration	$\mu mol\ m^{-2}\ s^{-1}$	3.63	5.20	3.26	76.58

Captions of Tables and Figures

Table 1. Default PFT-level, site-specific and optimized parameters for the PiTS site used in CLM 4.0. PFT-level parameters are for the temperate evergreen needleleaf forest (ENF) type. Optimized values were obtained using the pretreatment data (PRE_OPT), and for the transpiration data during the shading period (HS_MB). In the HS_MB optimization, only the mp and bp parameters were optimized, while other parameters retain their pretreatment optimization values.

Table 2. Pretreament state variables included in the optimization. Simulated values were obtained using the default parameters (PRE_STD) and the optimized parameters (PRE_OPT). The bias reduction (%) caused by the optimization is listed in the last column. In the case of leaf, root and aboveground biomass, we use allometric equations

1059 from multiple sources (Baldwin, 1987; Naidu et al., 1998; Vanlear et al., 1986) that went
1060 into producing a range. The bias calculation uses the mean of the range. For sap flow and
1061 soil respiration, daily observations were made, but the values represent a mean over the
1062 25 pretreatment days over both LS and HS periods. $\delta^{13}C$ values represent observed and
1063 simulated values on the day before treatments began.
1064 **Figure 1** (a) Air temperature (T, °C), relative humidity (Hr, %) and (b) wind speed (u, m
1065 s^{-1}) under the shade cloth at the top of the canopy compared with open field
1066 measurements at 2 m height; (c) Typical diurnal patterns of photosynthetically active
1067 radiation (PAR, μmol m^{-2} s^{-1}) at the site under full sun, light shade or heavy shade
1068 treatments.
1069 **Figure 2** (a) Daily air temperature (°C) and precipitation (mm d^{-1}) for the pretreatment
1070 and treatment of light shade (LS) and heavy shade (HS) (Day -20 to 25), (b) change in
1071 daily atmospheric long wave radiation (LW, W m^{-2}), short wave radiation (SW, W m^{-2})
1072 and $^{13}CO_2$ (PPMV) prior to and after exposure to shade treatments. Dashed gray line
1073 represents the starting day of the treatment.
1074 **Figure 3** (a) CLM simulated change of leaf carbon (PRE_STD_LeafC), stem carbon
1075 (PRE_STD_StemC) and root carbon (PRE_STD_RootC) with default parameters, and
1076 change of those (PRE_OPT_LeafC, PRE_OPT_StemC and PRE_OPT_RootC) simulated
1077 with optimized parameters for the pretreatment period between year 2003 and Sep. 1st
1078 (dashed gray line) of year 2010. Observational estimations of leaf (OBS_LeafC, which
1079 are 221.1 g C m^{-2}, 283.8 g C m^{-2} and 181.9 g C m^{-2}), stem (OBS_StemC, which are
1080 1011.2 g C m^{-2}, 973.8 g C m^{-2} and 1220.1 g C m^{-2}) and root (OBS_RootC, which is 488.4
1081 g C m^{-2}) are based on measured stem diameters at breast height and allometric

relationships from similarly aged loblolly pine (Baldwin, 1987; Naidu et al., 1998; Vanlear et al., 1986). Note that y-axis is log10-scaled. (b) Comparison of observed and simulated light response of top of the canopy leaves of loblolly pine at the PiTS-1 site. Solid black circles are mean ± 1 std dev of observations. Solid red and green circles are simulated results from the net photosynthesis module of the functional unit testing framework using site-observed parameters (PRE_STD) and optimized parameters (PRE_OPT), respectively (see section 2.2.2). Simulations are with the mean observed internal CO_2 concentrations (Ci) and leaf temperatures (Tleaf) at the observed light (PAR) levels and the site's observed leaf nitrogen (Na). Three grey bars represent the mean ± 1 std dev of midday PAR levels under the light shade treatment (LS), heavy shade treatment (HS) and open field condition (OF).

Figure 4 (a) Observed (obs) and CLM simulated (sim) daily soil temperature at 0-5cm depth (standard deviation, *SD* = 0.6-1.4 °C), (b) volumetric soil water content at 15-95cm depth (±*SD*) and (c) the transpiration before and after initiation of light shade (LS) or heavy shade (HS) treatments (*SD* = 0.1-1.7 mm day^{-1}). "HS – opt" represents the CLM simulation with optimized leaf conductance parameters. The vertical dashed lines indicate the starting day of the shade treatments.

Figure 5 (a) Observed (obs) and CLM simulated (sim) daily stem carbon relative to day 0 (±*SD*), and (b) soil respiration prior to and after exposure to light shade (LS) and heavy shade (HS) treatments (±*SD*). Both observed and simulated stem carbon were normalized to 1 at Day 0. The simulated soil respiration is the combination of autotrophic respiration from roots and heterotrophic respiration from the decay of litter and soil organic matter. The vertical dashed lines indicate the starting day of the treatments.

Figure 6 (a) Observed (black) and CLM simulated (blue) change in $\delta^{13}C$ (parts per thousand (‰)) of (a) leaf, (b) phloem, (c) bulk root and (d) soil surface efflux $\delta^{13}C$ for the light shade (LS, open circle) and heavy shade (HS, filled circle) pretreatment and treatment periods (± standard error (SE)). The modeled $\delta^{13}C$ values were calculated from the CLM simulated ^{13}C and ^{12}C variables and the reference standard (0.0112372) using the equation described in https://en.wikipedia.org/wiki/Δ13C. The $^{13}CO_2$ labeling pulse was initiated on Sep. 1st in year 2010 (Day 0). Dashed gray line represents the starting day (again Day 0) of the shading treatment. To better visualize the model results, inset figures illustrate the CLM simulated $\delta^{13}C$ values for the light shade (open triangle) and heavy shade (filled triangle) treatments from Day 1 to Day 25.

Figure 7. Conceptual model of label transport, assuming a constant velocity (V) of phloem stream with a cross-sectional area for the phloem pathway that varies as a function of ongoing photosynthetic rate. Cross-sectional area is conceptualized here as a varying number of similar phloem elements, with white elements in an active state, and dark elements inactive. The experimental case with a higher photosynthetic rate for the LS treatment and lower photosynthetic rate for the HS treatment is illustrated. Flux from roots (F_R) includes root respiration, root exudation, and turnover of root tissue. The entire label is assumed to exit the leaf and enter the active phloem stream, at a rate that is independent of the ongoing rate of photosynthesis, as observed in the experiment.

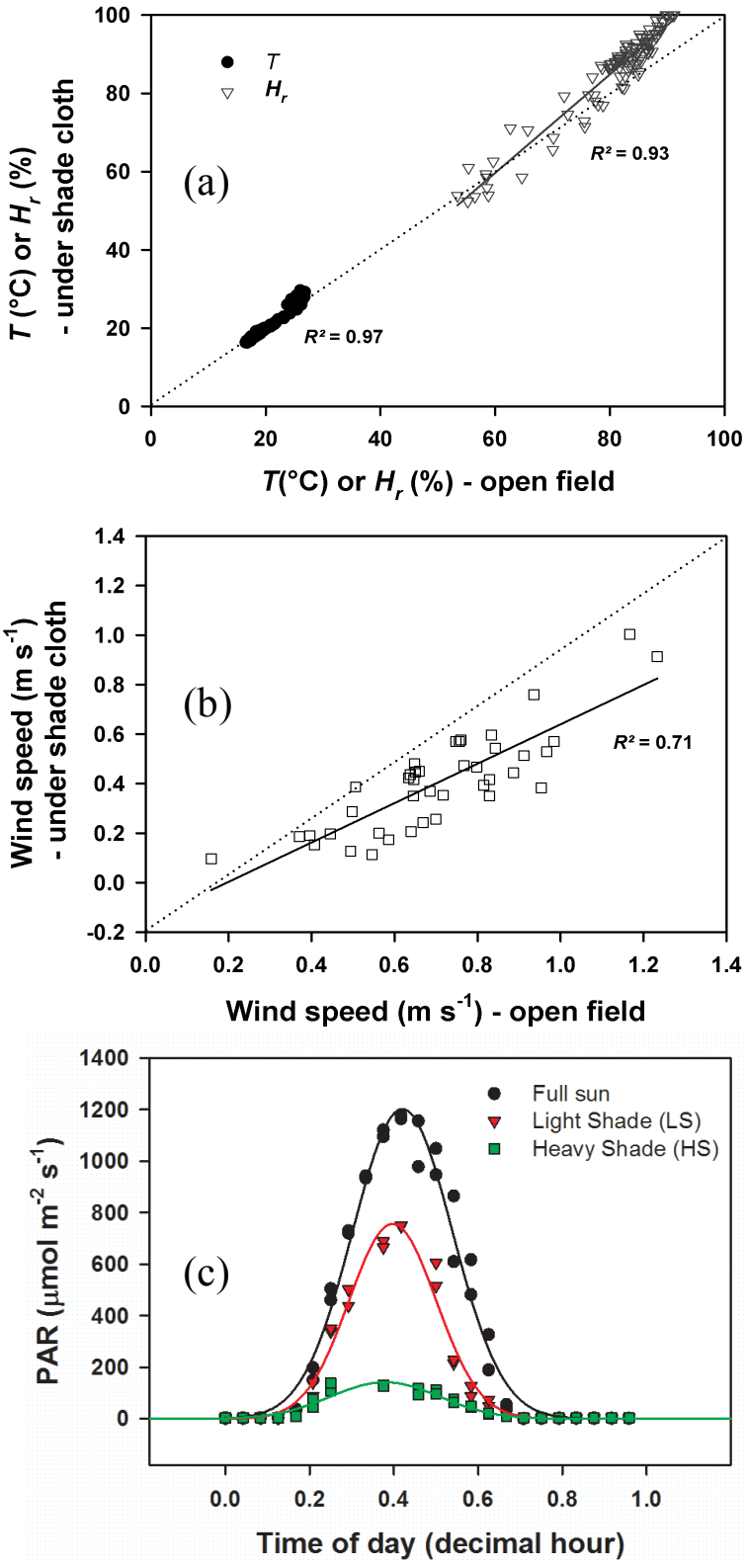

Figure 1 (a) Air temperature (T, °C), relative humidity (Hr, %) and (b) wind speed (u, m s^{-1}) under the shade cloth at the top of the canopy compared with open field measurements at 2 m height; (c) Typical diurnal patterns of photosynthetically active radiation (PAR, µmol m^{-2} s^{-1}) at the site under full sun, light shade or heavy shade treatments.

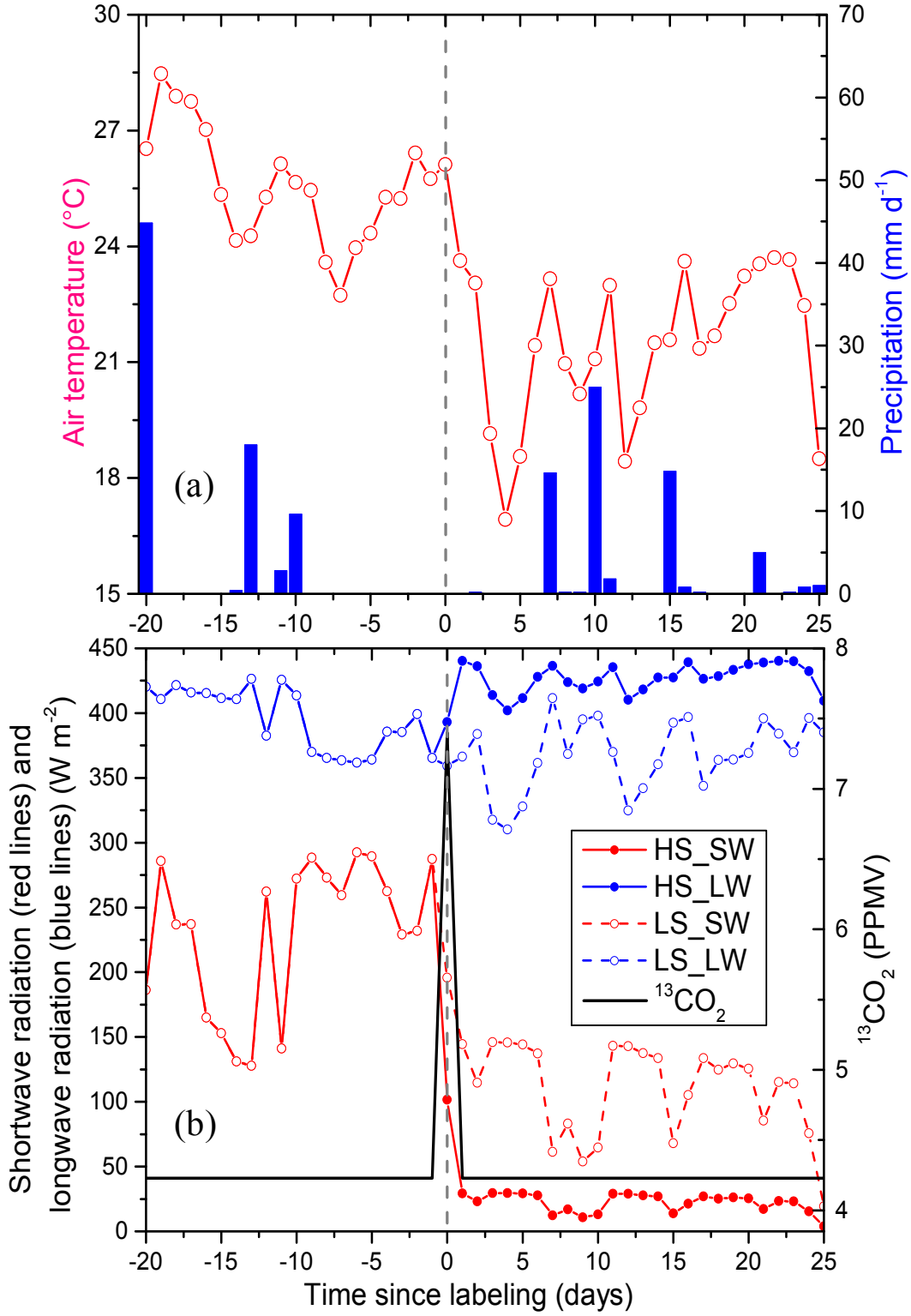

Figure 2 (a) Daily air temperature (°C) and precipitation (mm d^{-1}) for the pretreatment and treatment of light shade (LS) and heavy shade (HS) (Day -20 to 25), (b) change in daily atmospheric long wave radiation (LW, W m^{-2}), short wave radiation (SW, W m^{-2}) and $^{13}CO_2$ (PPMV) prior to and after exposure to shade treatments. Dashed gray line represents the starting day of the treatment.

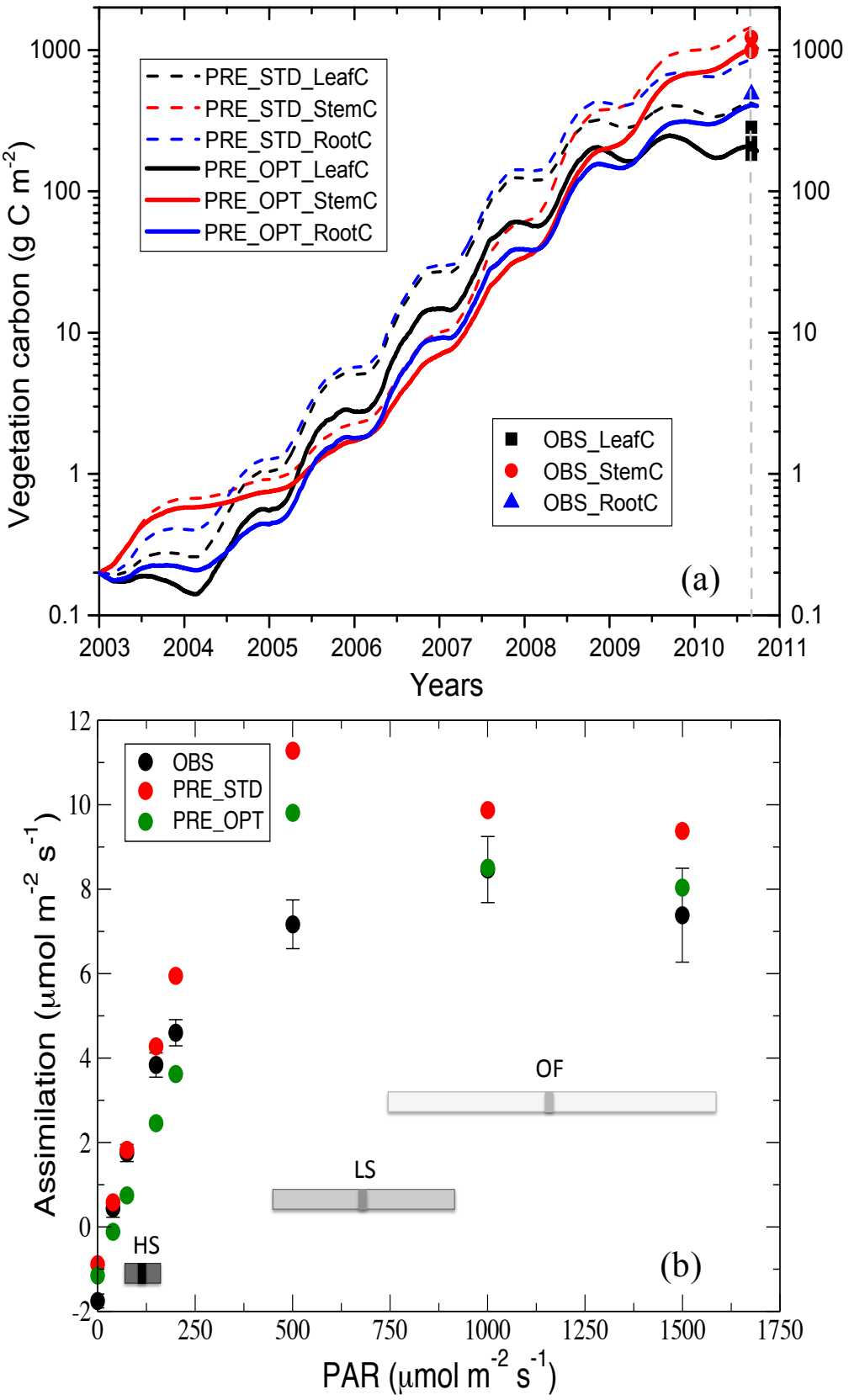

Figure 3 (a) CLM simulated change of leaf carbon (PRE_STD_LeafC), stem carbon (PRE_STD_StemC) and root carbon (PRE_STD_RootC) with default parameters, and change of those (PRE_OPT_LeafC, PRE_OPT_StemC and PRE_OPT_RootC) simulated with optimized parameters for the pretreatment period between year 2003 and Sep. 1st

(dashed gray line) of year 2010. Observational estimations of leaf (OBS_LeafC, which are 221.1 g C m^{-2}, 283.8 g C m^{-2} and 181.9 g C m^{-2}), stem (OBS_StemC, which are 1011.2 g C m^{-2}, 973.8 g C m^{-2} and 1220.1 g C m^{-2}) and root (OBS_RootC, which is 488.4 g C m^{-2}) are based on measured stem diameters at breast height and allometric relationships from similarly aged loblolly pine (*Baldwin*, 1987; *Naidu et al.*, 1998; *Vanlear et al.*, 1986). Note that y-axis is log10-scaled. (b) Comparison of observed and simulated light response of top of the canopy leaves of loblolly pine at the PiTS-1 site. Solid black circles are mean ± 1 std dev of observations. Solid red and green circles are simulated results from the net photosynthesis module of the functional unit testing framework using site-observed parameters (PRE_STD) and optimized parameters (PRE_OPT), respectively (see section 2.2.2). Simulations are with the mean observed internal CO_2 concentrations (Ci) and leaf temperatures (Tleaf) at the observed light (PAR) levels and the site's observed leaf nitrogen (Na). Three grey bars represent the mean ± 1 std dev of midday PAR levels under the light shade treatment (LS), heavy shade treatment (HS) and open field condition (OF).

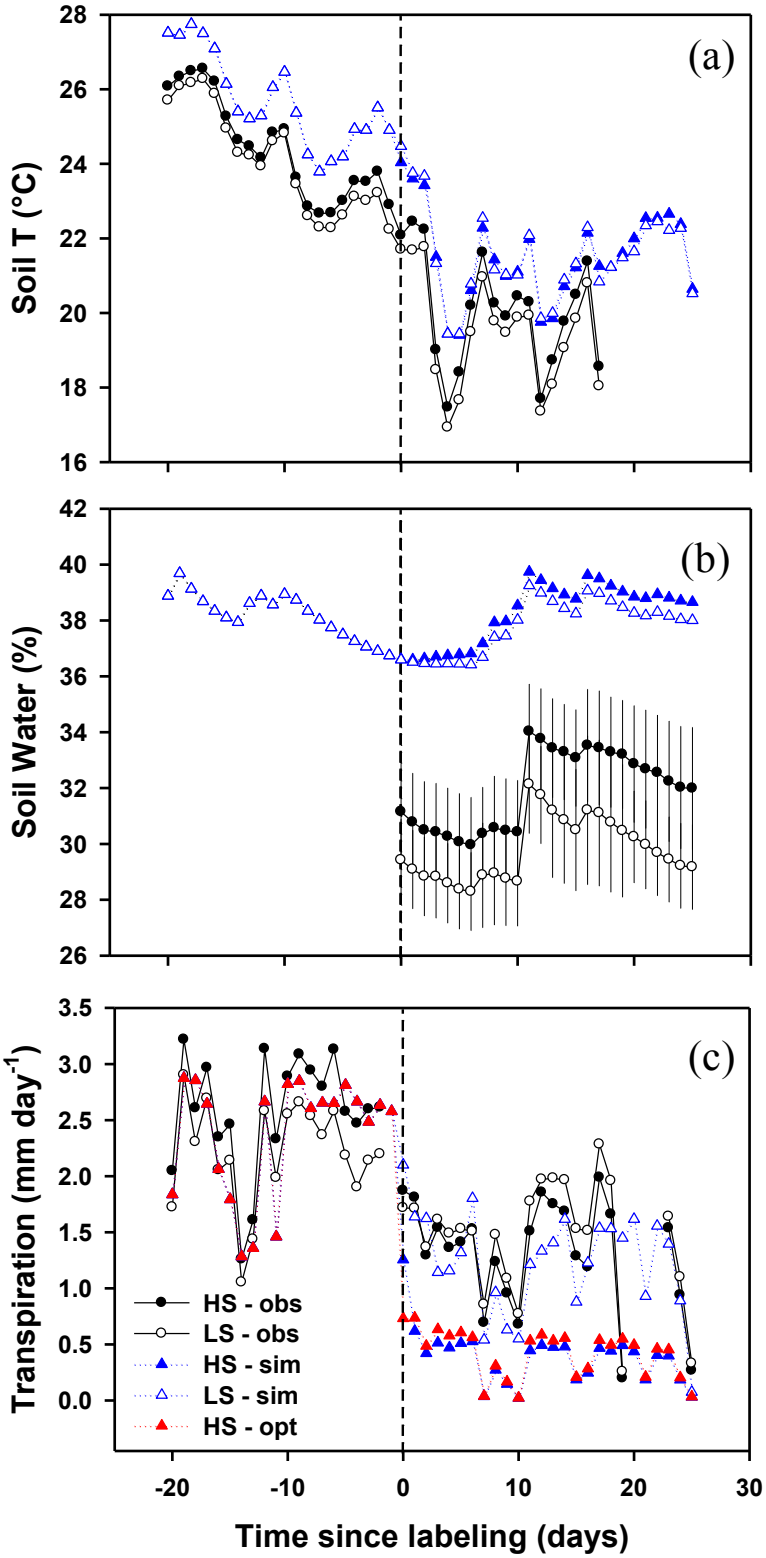

Figure 4 (a) Observed (obs) and CLM simulated (sim) daily soil temperature at 0-5cm depth (standard deviation, *SD* = 0.6-1.4 °C), (b) volumetric soil water content at 15-95cm depth (±*SD*) and (c) the transpiration before and after initiation of light shade (LS) or heavy shade (HS) treatments (*SD* = 0.1-1.7 mm day^{-1}). "HS – opt" represents the CLM simulation with optimized leaf conductance parameters. The vertical dashed lines indicate the starting day of the shade treatments.

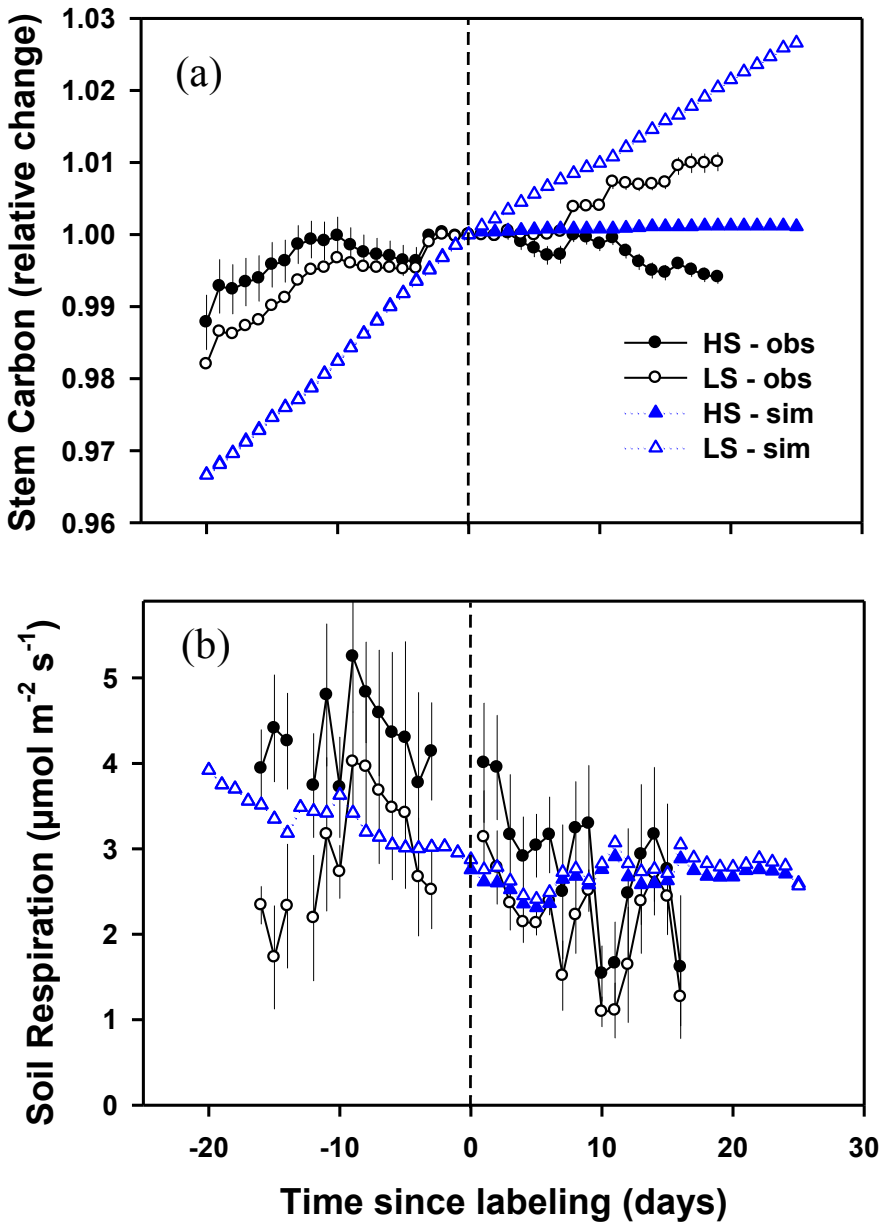

Figure 5 (a) Observed (obs) and CLM simulated (sim) daily stem carbon relative to day 0 (±*SD*), and (b) soil respiration prior to and after exposure to light shade (LS) and heavy shade (HS) treatments (±*SD*). Both observed and simulated stem carbon were normalized to 1 at Day 0. The simulated soil respiration is the combination of autotrophic respiration from roots and heterotrophic respiration from the decay of litter and soil organic matter. The vertical dashed lines indicate the starting day of the treatments.

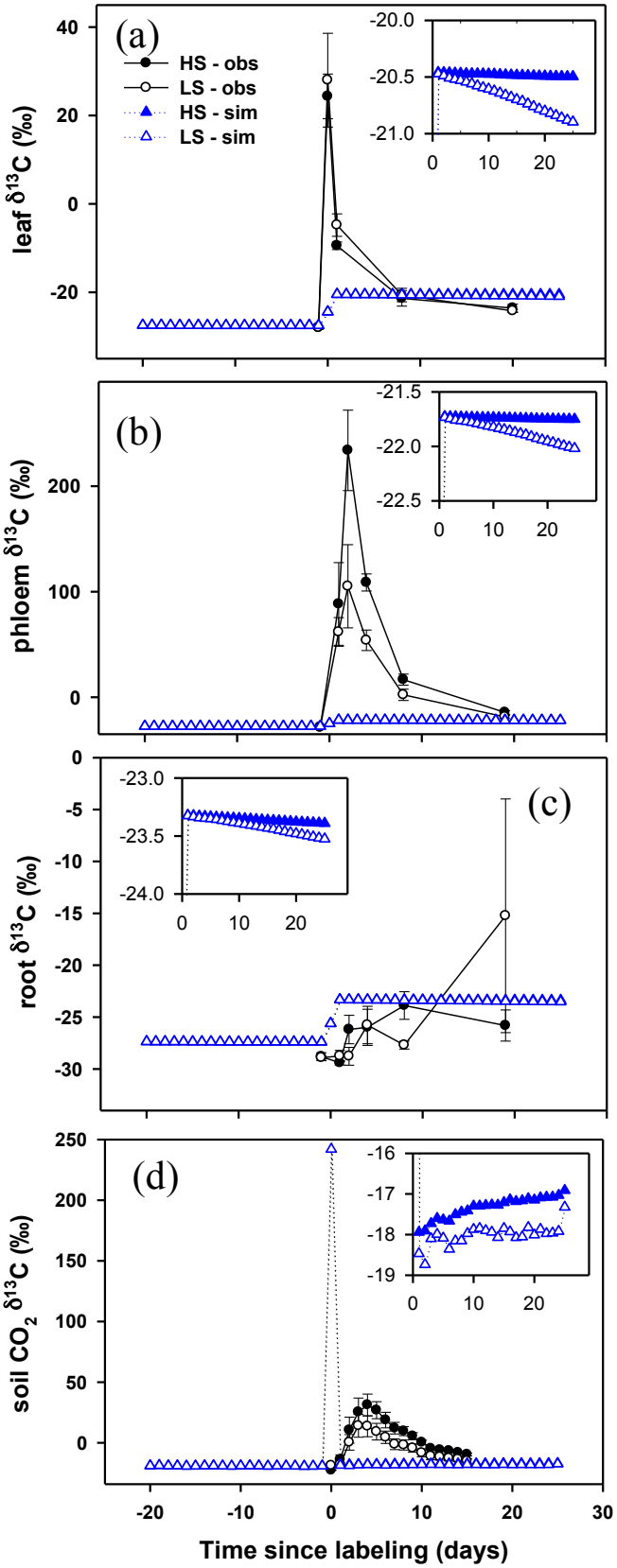

Figure 6 (a) Observed (black) and CLM simulated (blue) change in $\delta^{13}C$ (parts per thousand (‰)) of (a) leaf, (b) phloem, (c) bulk root and (d) soil surface efflux $\delta^{13}C$ for the light shade (LS, open circle) and heavy shade (HS, filled circle) pretreatment and treatment periods (± standard error (SE)). The modeled $\delta^{13}C$ values were calculated from the

CLM simulated ^{13}C and ^{12}C variables and the reference standard (0.0112372) using the equation described in https://en.wikipedia.org/wiki/Δ13C. The $^{13}CO_2$ labeling pulse was initiated on Sep. 1st in year 2010 (Day 0). Dashed gray line represents the starting day (again Day 0) of the shading treatment. To better visualize the model results, inset figures illustrate the CLM simulated $\delta^{13}C$ values for the light shade (open triangle) and heavy shade (filled triangle) treatments from Day 1 to Day 25.

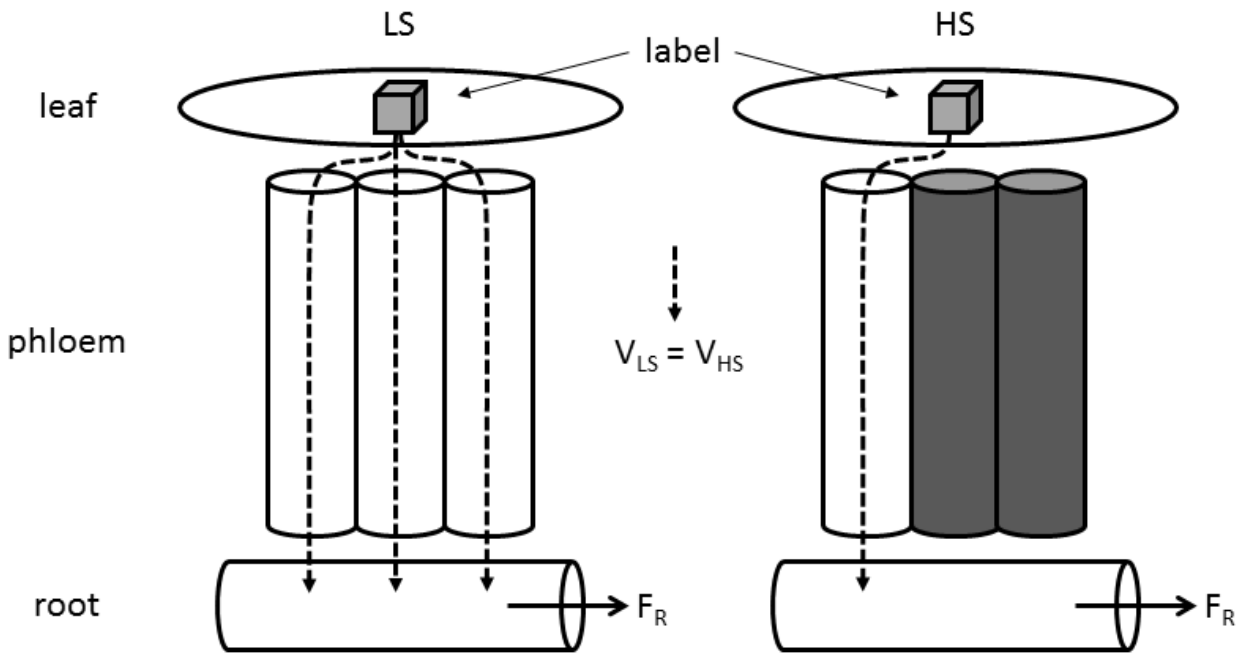

Figure 7. Conceptual model of label transport, assuming a constant velocity (V) of phloem stream with a cross-sectional area for the phloem pathway that varies as a function of ongoing photosynthetic rate. Cross-sectional area is conceptualized here as a varying number of similar phloem elements, with white elements in an active state, and dark elements inactive. The experimental case with a higher photosynthetic rate for the LS treatment and lower photosynthetic rate for the HS treatment is illustrated. Flux from roots (F_R) includes root respiration, root exudation, and turnover of root tissue. The entire label is assumed to exit the leaf and enter the active phloem stream, at a rate that is independent of the ongoing rate of photosynthesis, as observed in the experiment.